

Advances in the Development of Granular Microporous Injectable Hydrogels with Non-spherical Microgels and Their Applications in Tissue Regeneration

Haiyan Li,* Keerthi Subramanian Iyer, Lei Bao, Jiali Zhai, and Jiao Jiao Li

Granular microporous hydrogels are emerging as effective biomaterial scaffolds for tissue engineering due to their improved characteristics compared to traditional nanoporous hydrogels, which better promote cell viability, cell migration, cellular/tissue infiltration, and tissue regeneration. Recent advances have resulted in the development of granular hydrogels made of non-spherical microgels, which compared to those made of spherical microgels have higher macroporosity, more stable mechanical properties, and better ability to guide the alignment and differentiation of cells in anisotropic tissue. The development of these hydrogels as an emerging research area is attracting increasing interest in regenerative medicine. This review first summarizes the fabrication techniques available for non-spherical microgels with different aspect-ratios. Then, it introduces the development of granular microporous hydrogels made of non-spherical microgels, their physicochemical characteristics, and their applications in tissue regeneration. The limitations and future outlook of research on microporous granular hydrogels are also critically discussed.

1. Introduction

1.1. Traditional Hydrogels and Their Limitations

A hydrogel is a 3D network of hydrophilic polymers that swells in water and holds a large amount of liquid while maintaining a solid structure. Monolithic hydrogels are composed of crosslinked hydrophilic polymers,^[1] which have macromolecular structures comprising covalently bonded repeated monomer units. Before the polymers are crosslinked, they can interact with liquid and form “hydrosol” which is not a solid 3D structure. The process of crosslinking forms covalently bonded polymer chains, which converts the “hydrosol” into “solid hydrogel” with entangled polymer chains and an insoluble solid 3D network. During crosslinking, voids form between entangled polymer chains, which contribute to forming the porous structure


of hydrogels. Due to the inherent properties of covalent bonds, the voids between polymer chains are usually in the nanoscale range (mean pore size ≈ 5 nm), leading to the formation of traditional hydrogels with nanoporous structures.^[2]

For many years, traditional nanoporous hydrogels have been used in a wide variety of biomedical applications, including drug delivery, tissue engineering, wound dressing, and trauma healing, among others with dramatic increases in market value. Allied Market Research has reported that the global hydrogel market was valued at \$22.1 billion in 2019, and is projected to reach \$31.4 billion by 2027, growing at a CAGR of 6.7% from 2020 to 2027.^[3] Hydrogels have been widely applied as drug delivery systems, due to their nanoporous structure that is suitable for encapsulating drugs or bioactive molecules.^[4] In addition to conventional noninjectable hydrogels, injectable hydrogels have recently attracted more attention in biomedical applications.^[5] These injectable hydrogels can be made to have common hydrogel characteristics of biocompatibility, tunable biodegradability and mechanical properties, permeability to oxygen and nutrients, and properties mimicking native extracellular matrix (ECM), as well as having the practical advantages of minimally invasive delivery and ease of handling and manipulation. For these reasons, they have been extensively studied as tunable biomaterial scaffolds or carriers of cells and bioactive molecules for applications in tissue repair and regeneration.^[6] However, when

H. Li, K. S. Iyer, L. Bao
Chemical and Environment Engineering Department
School of Engineering
STEM College
RMIT University
124 La Trobe Street, Melbourne, VIC 3001, Australia
E-mail: haiyan.li4@rmit.edu.au

J. Zhai
School of Science
STEM College
RMIT University
124 La Trobe Street, Melbourne, VIC 3001, Australia

J. J. Li
School of Biomedical Engineering
Faculty of Engineering and IT
University of Technology Sydney
Sydney, NSW 2007, Australia

 The ORCID identification number(s) for the author(s) of this article can be found under <https://doi.org/10.1002/adhm.202301597>

© 2023 The Authors. Advanced Healthcare Materials published by Wiley-VCH GmbH. This is an open access article under the terms of the Creative Commons Attribution License, which permits use, distribution and reproduction in any medium, provided the original work is properly cited.

DOI: 10.1002/adhm.202301597

injectable hydrogels are used as cell delivery systems, increasing studies have shown that their nanoporous structure cannot maintain the normal behavior and function of encapsulated cells, such as cell spreading, migration, proliferation, differentiation, and cell–cell communication, as the micron-sized cells are much larger than the nanoscale pores of the hydrogels.^[7] Thus, the nanoporous structure of traditional hydrogels imposes physical constraints on encapsulated cells, which interferes with hydrogel function by inhibiting stem cell proliferation and delaying new matrix deposition.^[7b,c] It has been widely reported that cells usually present a round morphology and proliferate slowly when encapsulated in traditional nanoporous hydrogels.^[7b,8] In addition, the encapsulated cells tend to form aggregates and display significantly impaired differentiation, as well as limited cell-cell communications, all of which impede normal cell behavior and function.^[8c,9]

More recently, the concept of “in vivo” tissue engineering has led to the development of cell-free hydrogels for enhancing tissue regeneration.^[10] In vivo tissue engineering promises to break the bottleneck of traditional tissue engineering technology by only using cell-free biomaterial scaffolds to recruit in situ host cells and induce tissue ingrowth into scaffolds to enable tissue regeneration, taking advantage of the surrounding microenvironment as a natural bioreactor.^[10,11] As the only and key factor, the engineered biomaterial scaffolds for in vivo tissue engineering require specific biophysical and biochemical cues to direct endogenous cells to the injury site and modulate the behavior of these cells. So far, various traditional injectable hydrogels have been designed to improve healing within a variety of tissue defects, as discussed in recent review papers.^[5b,12] However, increasing evidence suggests that the nanoporous structure of these traditional hydrogels presents obstacles for the ingrowth of surrounding cells and tissues, which can weaken the integration of implanted hydrogels into the host tissue and impede tissue regeneration.^[13]

Taken together, although existing injectable hydrogels have favorable properties as biomaterial scaffolds for in vitro and/or in vivo tissue engineering, particularly with their biocompatibility, biodegradability, tunability, and potential for minimally invasive delivery, they face critical challenges for translation to clinical applications. On the one hand, when nanoporous injectable hydrogels are used as cell delivery systems, the encapsulated cells cannot maintain normal behavior due to physical constraints and/or cannot survive for long enough within the hydrogel without adequate diffusion of nutrients and wastes. On the other hand, when used as cell-free scaffolds, nanoporous hydrogels are not able to recruit host cells or allow their penetration into the hydrogel structure due to the limits imposed by nanosized pores.^[14] Thus, it is not feasible to use the current nanoporous injectable hydrogels for practical applications in tissue regeneration.

1.2. Microporous Hydrogels

1.2.1. Advantages of Microporous Hydrogels

Recently, microporous hydrogels with pore sizes ranging between tens to hundreds of microns have emerged as a new biomaterial strategy to address the limitations imposed by traditional injectable hydrogels, since they combine the benefits

Table 1. Key differences between nanoporous and microporous hydrogels.

	Nanoporous hydrogel	Microporous hydrogel
Pore size ^[15]	≈5 nm	>50 μm
Mechanical stability ^[16]	Moderate	Enhanced
Cell morphology ^[17]	Round	Spread
Cell viability ^[2,18]	Limited	High
Cell migration ^[2,19]	Limited	High
Cell proliferation ^[17]	Low	High
Cell differentiation ^[1a]	Impaired	Normal
Cell and tissue infiltration ^[14c,16b,18,19,20]	Limited	Enhanced

of traditional 3D microporous pre-formed scaffolds and traditional injectable nanoporous hydrogels. With their microscale pores, microporous hydrogels have unique advantages compared to nanoporous hydrogels, with key differences listed in **Table 1**. When used as cell-delivery vehicles for in vitro tissue engineering, microporous hydrogels do not impose physical restraints on encapsulated cells and facilitate efficient diffusion of nutrients/wastes, leading to normal cell morphology, high cell viability, and normal cell differentiation. When used as cell-free scaffolds for in vivo tissue engineering, their microscale pores can enhance the infiltration of recruited endogenous cells and ingrowth of blood vessels, leading to improved tissue regeneration. In addition, microporous hydrogels have a more tunable internal structure and controllable biodegradability compared to nanoporous hydrogels.

1.2.2. Strategies for Developing Microporous Hydrogels

Although different strategies exist for fabricating microporous hydrogels, it is still challenging to obtain injectable microporous hydrogels. Two main strategies have been reported to create a microporous structure of injectable hydrogels for enhancing the infiltration of cells and tissue: 1) accelerating degradation of the implanted hydrogels in vivo; 2) fabricating microporous injectable hydrogels in vitro before implantation. The basic principle, advantages and disadvantages of each strategy are listed in **Table 2**. Accelerating the hydrogel degradation and applying a lightly crosslinked hydrogel can create space after hydrogel implantation to benefit the infiltration of cells and tissue, but this strategy still faces some major challenges.^[21] Recently, injectable hydrogels with microscale pores have been developed to address existing challenges, among which microgel assembly methods have attracted increasing attention.^[7b,17,20,22] Some interesting examples include a novel “triggered micropore-forming” bioprinting method developed by Li and Mongeau’s group in 2020, which was used to print microporous viscoelastic hydrogels.^[23] The printing mechanism was based on stimuli-triggered microphase separation to form interconnected cell-sized pores. This method could provide fine control over the structure, pore size, porosity, viscoelasticity, and mechanical properties of the printed hydrogels. The hydrogels showed microporous structure, as well as high permeability and toughness which not only enabled the proliferation and migration of encapsulated cells but also the regeneration of mechanically dynamic tissues.

Table 2. An overview of methods utilized for fabricating injectable microporous hydrogels.

Fabrication Strategy	Basic principle	Advantages	Disadvantages
Adjust the degradation of hydrogels ^[21a-h]	Chemically modify the materials used for making hydrogels to accelerate their degradation <i>in vivo</i>	-No advanced fabrication methods needed -Clear degradation mechanism -Cost-effective	-Uncertain degradation rate <i>in vivo</i> -Uncertain porous structure -Uncertain cytotoxicity of the modified materials
Microgel assembly ^[15a,16b,17,19b,20,24]	Produce microgels with different methods and assembly the microgels into a 3D bulk hydrogel	-Tunable mechanical and physical properties -Can predict the porous structure -No additional chemicals involved -No change to the materials	-Advanced fabrication techniques needed -Can be costly

1.2.3. Accelerating Hydrogel Degradation

Initial approaches to developing microporous hydrogels consisted of accelerating the *in vivo* degradation of injectable hydrogels to create large voids in the hydrogel as early as possible following implantation, to facilitate the infiltration of endogenous cells and tissue.^[21a,f,g] For example, oxidizing sodium alginate (SA) can accelerate the degradation of SA hydrogel by promoting hydrolysis, whereby the oxidized SA exhibits a faster degradation rate and contains more reactive groups compared to native SA.^[21f,g] Additionally, enzymatically degradable hydrogels have recently been developed by crosslinking the material with a matrix metalloproteinase (MMP) sensitive peptide crosslinker which can be specifically cleaved by cells. After implantation, the endogenous MMP secreted by cells can react with the peptide crosslinkers to accelerate hydrogel degradation, resulting in large pores within the hydrogels.^[21b,h,i]

Although the strategy of accelerating hydrogel degradation *in vivo* shows promise, its application is limited in several aspects. First, chemical modifications made to native hydrogel materials introduce extra chemical groups, which may alter the biocompatibility of the hydrogel. For example, the oxidation process of SA introduces aldehyde groups, posing a potential risk to the biocompatibility of SA. Second, it is difficult to monitor and control the process by which the microporous structure of implanted hydrogels forms *in vivo* from degradation, which prevents the specific design of hydrogel features based on *in vivo* results. For example, a study on enzymatically degradable SA hydrogels found only a slight improvement in tissue infiltration in the modified hydrogel (16.3%) compared to the control (12.7%).^[21b] Thus, despite the potential benefits of this strategy in accelerating degradation to create space within the hydrogel following *in vivo* implantation, significant challenges still need to be addressed.

1.2.4. Microgel Assembly

Recently, microgel assembly has emerged as a new strategy to obtain microporous injectable hydrogels, tackling the abovementioned challenges of chemical modification to increase hydrogel degradation.^[16c,18,20,25] Using this method, various hydrogel materials can be used in their native form without additional modification, and the structure of resulting microporous injectable hydrogels can be characterized *in vitro*, and hydrogel properties can be further adjusted if necessary, according to the results of *in*

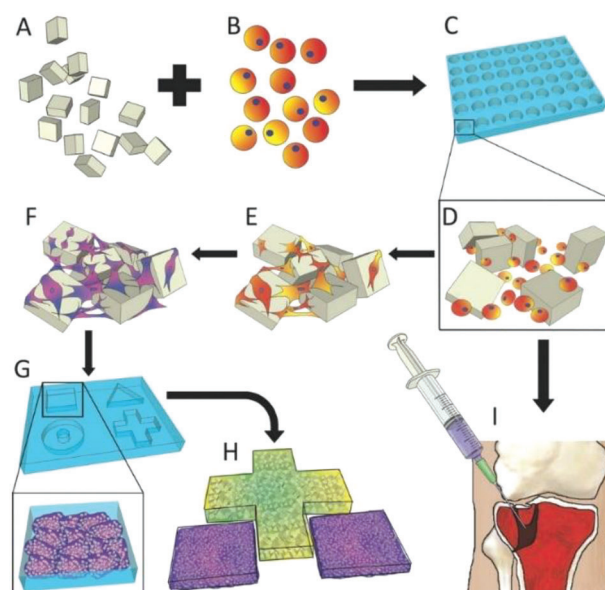


Figure 1. Schematic representation of bottom-up tissue engineering approach with microgels. A) Microgels. B) Cells. C) Micro-wells for culturing cells on microgels. D) Cells are cultured on the microgels. E, F) Cell proliferate and differentiate when they are cultured on the microgels *in vitro*. Cell fate can be affected by the properties of the microgels. G) Cell/microgel aggregates can be further cultured into larger-sized tissue constructs *in vitro*. H) Different tissue constructs can be combined to form controlled complex tissues. I) The mixed suspension of cells and microgels can also be directly injected into a defect site for *in vivo* tissue engineering. Reproduced with permission.^[25a] Copyright 2014, Wiley-VCH GmbH.

vitro experiments. The microgel assembly method includes two steps as shown in **Figure 1**: microgel production and microgel assembly. First, microgels are produced using various techniques (details will be discussed later), which are injected into tissue defects and become freely stacked in the defect area. Then, a second crosslinking step is introduced to assemble the freely stacked microgels into a bulk hydrogel. During this assembly process, the freely stacked microgels are fixed in position within the hydrogel and leave voids between them, since there is no extra force present to induce close arrangement of the microgels.

The voids that form during microgel assembly are usually in the microscale range, although the size of voids can be easily adjusted by tuning the size and density of the microgels. These voids provide sufficient space for cell spreading, proliferation,

Table 3. Key difference between microporous hydrogels comprising non-spherical microgels and those obtained from spherical microgels.

Hydrogel type	Pore shape	Pore size [μm]	Porosity [%]	Anisotropic cues	Mechanical flexibility	Cell behavior	Tissue regeneration
Microporous hydrogels comprising non-spherical microgels ^[7b,17,24c,25c]	Irregular with different shapes	20–300	High (≈90)	High	High	High cell viability, spread, proliferation, migration, alignment, and cell-cell interactions	High ECM synthesis and mechanical strength of regenerated tissue
Microporous hydrogels comprising spherical microgels ^[8b,19b]	Round	20–50	Low (30–50%)	No	Low	Relative low cell viability, proliferation, migration, alignment, and cell-cell interactions	Relative low ECM synthesis and mechanical strength of regenerated tissue

mass transport, and tissue ingrowth. Compared to nanoporous injectable hydrogels, microporous hydrogels have been shown to improve the infiltration of cells and tissues and enhance cell viability and proliferation *in vitro* and *in vivo*.^[15a,18,20,26]

1.3. Microporous Hydrogels Fabricated with Spherical or Non-spherical Microgels

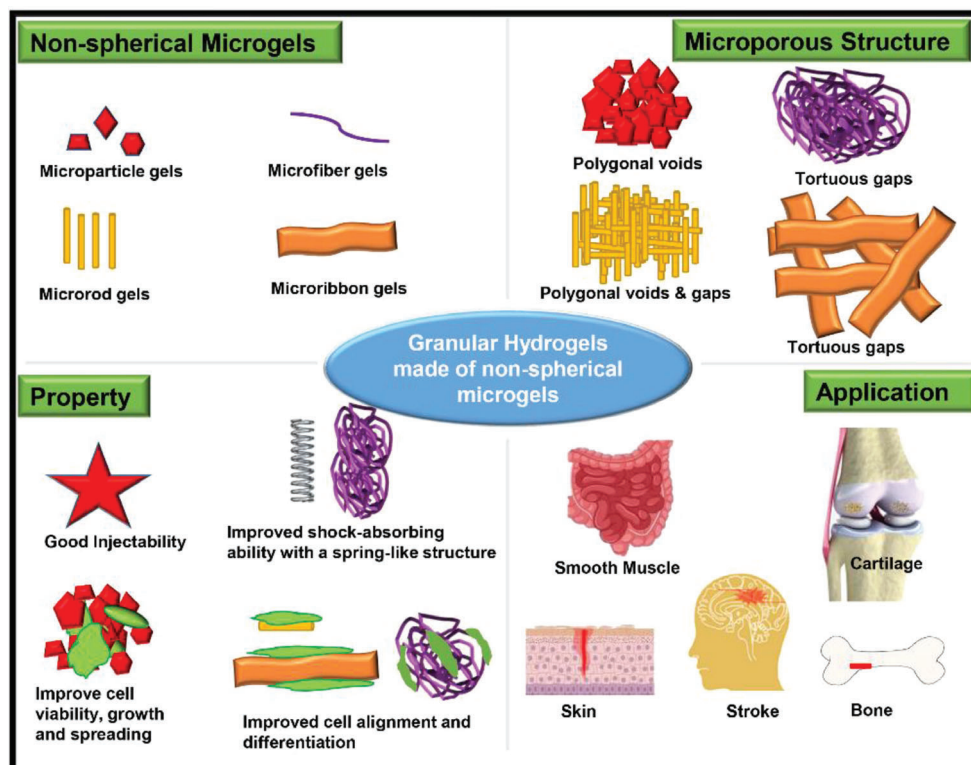
Microgel is a key factor in the fabrication of microporous hydrogels. As described above, the voids that form between microgels during assembly create space for cell and tissue infiltration.^[25a] Accordingly, the size and shape of voids are determined by the features of the microgels, including microgel size, shape, particle-to-volume fraction, and stiffness.^[15b,25a,27] Microgel properties have been shown to significantly influence the properties of the resulting bulk microporous hydrogels, and subsequently affect cell behavior and the outcomes of tissue regeneration.^[7b,15b,24c,27,28] Initially, microgels with a perfectly spherical shape were developed using existing techniques, which have been discussed in excellent review papers.^[15b,25b] Recently, microgels with different shapes have been developed, including spherical microgels, microparticulate gels, microrod gels, microribbon gels, and microfiber gels, among others, and are categorized according to their aspect-ratio (ratio of the gel's longest dimension to shortest dimension). The aspect-ratio of spherical microgels is about 1, while low-aspect-ratio microgels have an aspect ratio of 1–5 and high-aspect-ratio microgels are >5.^[17] **Table 3** summarizes the key differences between microporous hydrogels comprising non-spherical microgels and those obtained from spherical microgels.

Compared to microporous hydrogels made from spherical or low-aspect-ratio microgels, those made from high-aspect-ratio microgels have pore size and porosity that can better enhance cell viability, proliferation, and migration.^[7b,17] Thus, the hydrogels made of high-aspect-ratio microgels may also better direct the alignment and differentiation of cells to increase the formation of new tissue and provide more stable mechanical properties. For example, Sutarin et al. reported that the pore structure of microporous annealing particle (MAP) hydrogels can be enhanced by increasing the microgel aspect ratio. In MAP hydrogels, the mean pore size can increase from 39 to 82 μm and the porosity can significantly increase from 65 to 90% compared to hydrogels made from spherical or lower aspect-ratio rod-shaped microgels.^[7b] These high-aspect-ratio microporous hydrogels can

provide large empty spaces to improve cell ingrowth and cell–cell interactions.

Increasing studies have shown that the close-packed lattice of microporous hydrogels with spherical microgels limits interactions between individual microgels and precludes any anisotropy within the bulk hydrogel. Consequently, these hydrogels cannot provide important guidance cues to align cells of anisotropic tissues whose properties vary in three dimensions, such as muscle and tendon.^[16c,24c,25c] For example, muscles comprise muscle fibers that are parallel to the long axis, and tendons also have collagen fibers that are longitudinally arranged in a hierarchical manner. In the majority of tissues in the human body, their organization and matrix pores are not symmetrical or spheroidal, but rather irregular with high aspect-ratio structures.^[29] The problem of mimicking or repairing these anisotropic tissues can be addressed using microporous hydrogels made of high aspect-ratio microgels, which allow the formation of anisotropic structures within the bulk hydrogel to guide cell alignment and differentiation. It has been reported that a microporous hydrogel made of aligned high-aspect-ratio microribbons induced high viability, rapid adhesion, and alignment of smooth muscle cells, as well as supported the retention of smooth muscle contractile phenotype and accelerated uniaxial deposition of new matrix along the microribbons.^[24c] Another important feature of microporous hydrogels comprising high-aspect-ratio microgels is the significantly boosted flexibility and mechanical stability due to their spring-mimic structure. For instance, microporous hydrogels made of aligned high-aspect-ratio microribbons could sustain up to 90% strain and 3 MPa stress without failing, which enhanced the proliferation of human adipose-derived stromal cells by up to 30-fold within 3 weeks of culture.^[24a] In another study, microporous hydrogels with high-aspect-ratio microgels significantly increased the total amount of neocartilage produced by mesenchymal stem cells (MSCs) *in vitro*.^[15a] Because of their advantageous features, microporous hydrogels comprising non-spherical particularly high-aspect-ratio microgels have emerged as an area of heightened interest, which will be the focus of this review with a concentration on technologies for producing non-spherical microgels and current applications of the resulting microporous hydrogels (**Scheme 1**).

Several papers have reviewed microgels, microgel-based granular hydrogels, and their biomedical applications.^[14b,28a,30] For example, a recent review in 2022 discussed the microgel assembly method for fabricating microporous hydrogels,^[14b] with a primary focus on the fabrication and characteristics of microporous



Scheme 1. Microporous granular hydrogels: their assembly non-spherical microgels, structure, properties, and applications.

granular hydrogels based on various types of microgels. However, the fabrication techniques of microgels, especially high-aspect-ratio microgels developed using new techniques such as microribbons, microfibers, and microrods have not yet been reviewed in detail. Despite limited reports, these microgel designs deserve more attention due to their attractive properties in enabling anisotropic tissue regeneration.^[7b]

Filling the gap from existing reviews, the first part of this paper focuses on the techniques for fabricating non-spherical microgels, such as microrod, microribbon, microstrand, and microfiber gels. Then, we introduce the types of microporous hydrogels fabricated by assembling various non-spherical microgels, specifically discussing their physiochemical properties and guidance effects on cell behavior. Finally, we survey recent applications of these microporous hydrogels in different tissue regeneration applications. The content of this review is summarized in the Scheme. This review deliberates the current state-of-the-art on microporous injectable hydrogels made of nonspherical microgels, mostly focusing on experimental studies published in the last 5 years and giving a comprehensive account of the limited literature currently available on this topic, separated into the fabrication, properties, and application aspects.

2. Techniques for Fabricating Non-spherical Microgels

Spherical microgels were the first type of microgels developed to form microporous hydrogels based on microgel assembly, which have been widely used for the delivery of cells and drugs in

biomedical applications. Various techniques have been used to produce spherical microgels, including emulsion, microfluidic-based methods, electrohydrodynamic spraying, stereolithography, mechanical fragment method, wet spinning, and their combinations.^[16a,18,20,24c,25b,c,26a,31] Techniques including batch emulsion, microfluidics, and electrohydrodynamic spraying have recently become well-established, creating spherical microgels with high monodisperse features.^[15b,16b,25c,26a,31a,e,32] The principle, advantages, and limitations of these three technologies for producing spherical microgels have been introduced in three excellent review papers by Liu et al., Daly et al., and Kamperman et al., respectively.^[25b,31a,c] A major issue of existing techniques for fabricating spherical microgels is poor scalability, since they usually involve oils and chemical additives, and/or are restricted to polymer solutions with low viscosity.^[25b]

The well-established microfluidic-based methods, stereolithography, and mechanical fragment method have been adapted to produce non-spherical microgels with low-aspect-ratio, such as microparticulate gels and microrod gels.^[21a,31e,33] To meet the demand of producing non-spherical microgels with high-aspect-ratio, the wet spinning technique has attracted increasing attention and has been used to fabricate new morphologies such as microfibers and microribbons.^[15a,16a,c,20,24a,c,34] In addition, the mechanical fragment method has been adapted to segment nanoporous hydrogels into microstrands gels.^[25c] In this part, we will first introduce the techniques for fabricating non-spherical microgels with low-aspect-ratio, followed by methods for producing microgels with high-aspect-ratio and the properties of the microgels.

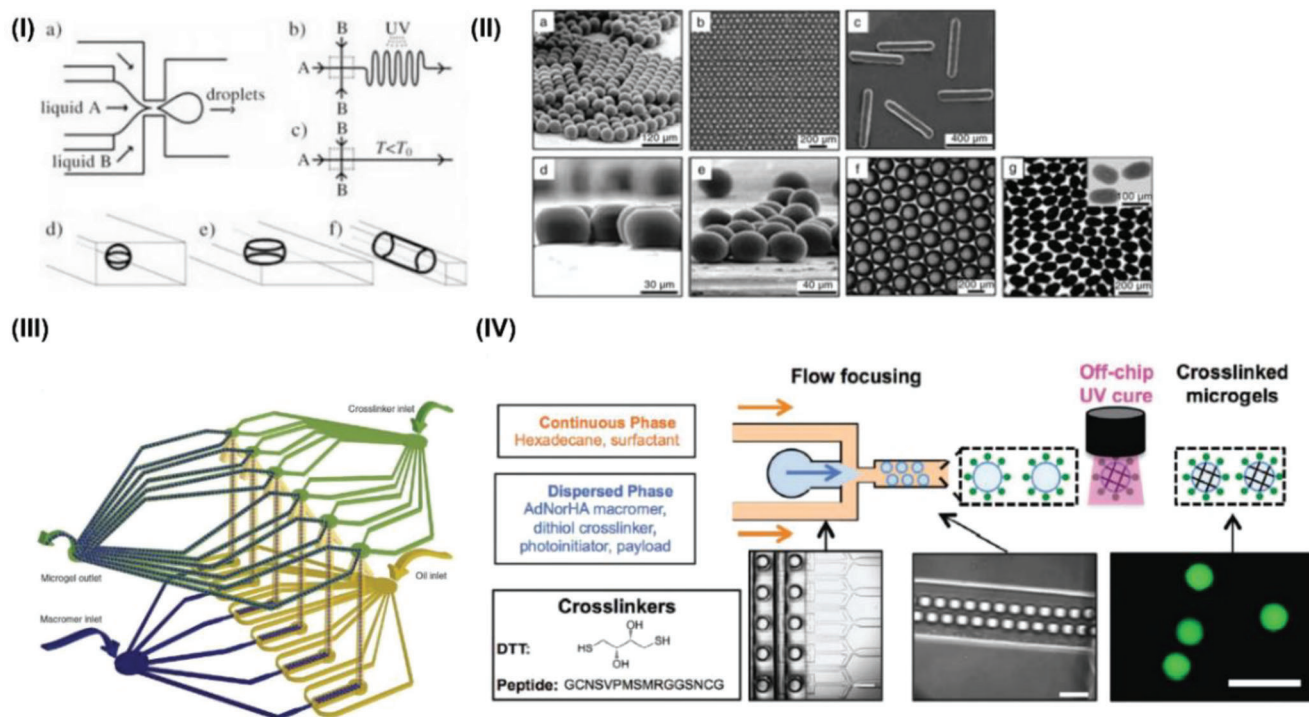


Figure 2. Microfluidic-based techniques for producing non-spherical microgels. I) Microfluidic flow-focusing device. II) Optical microscopy images of microgels obtained with the MFFD method. I,II) Reproduced with permission.^[33a] Copyright 2005, Wiley-VCH GmbH. III) A parallel droplet generator on a two-layer elastomer device. Reproduced under the terms of the Creative Commons CC-BY license.^[16b] Copyright 2018, The Authors, published by Springer Nature. IV) A novel parallelized step emulsification device to provide high throughput microgel generation. Reproduced with permission.^[26b] Copyright 2018, Wiley-VCH GmbH.

2.1. Techniques for Fabricating Nonspherical Microgels with Low-Aspect-Ratio

2.1.1. Microfluidic-Based Techniques

Figure 2 illustrates the mechanism of microfluidic-based techniques for fabricating non-spherical microgels. Xu et al. were the first to propose a general microfluidic technique to obtain microparticles with different shapes, through the use of a microfluidic flow-focusing device (MFFD) that can produce both spherical and non-spherical microgels^[33a] (Figure 2I). Briefly, two immiscible liquids with one being the continuous phase and the other being the disperse phase are forced into a narrow orifice, where the inner disperse phase liquid breaks due to water-in-oil or oil-in-water emulsification. During this process, monodisperse droplets form and are dispensed into the outlet channel where the droplets are crosslinked or solidified. The final shape of microgels is determined by the volume of the droplet controlled by the flow rate of the continuous and disperse phases, and the cross-sectional area of the outlet microchannel. If spherical microgels or microparticles are desired, the diameter of the spherical droplets given by $d_s = (6V/\pi)^{1/3}$ should be smaller than the height and width of the microchannel. If the diameter of the spherical droplets is larger than any dimension of the outlet microchannel, non-spherical microgels or microparticles can be obtained, such as those in the shape of a disk, ellipsoid, or rod, as shown in Figure 2II.^[33a] To ensure sufficient polymerization, droplets are crosslinked in elongated channels to allow longer

duration of exposure of the droplets to the crosslinking media. Headen et al. used a MFFD to produce 4-arm PEG maleimide (PEG-4MAL)-based droplets, and subsequently crosslinked the droplets with small molecule dithiothreitol to produce cell- and cell aggregate-laden synthetic PEG-4MAL-based microgels.^[31e]

To tackle the limits of low throughput and poor scalability of standard flow-focusing microfluidic techniques used to produce monodisperse microgels, several parallelized flow-focusing devices have been developed. For example, Headen et al. designed a parallel droplet generator on a two-layer elastomer device (Figure 2III), which has 600% increased throughput compared to single-nozzle devices.^[16b] Briefly, on the lower layer of the device, there are six channels for macromer precursor (and optionally cells) to flow through and another six channels for oil to flow through. Droplets are created and emulsified in oil when the macromer precursor and the oil meet and co-flow through a flow-focusing geometry. Then, the droplets generated in all six flow-focusing nozzles are carried up to the six merging points of the top layer of the device to be crosslinked, by the flow of crosslinker through 12 channels to the merging points. Following this, the crosslinked microgels flow from the six meeting points, through 12 channels and are collected in one pool before they exit the device at a single outlet. Microgels produced on parallel nozzles are equivalent to those produced on single nozzles with substantially the same polydispersity, and cell-laden microgels can also be produced with this method. Additionally, Jeong et al. developed a 3D monolithic elastomer device (3D MED) for mass production of monodisperse emulsion droplets.^[35] Briefly,

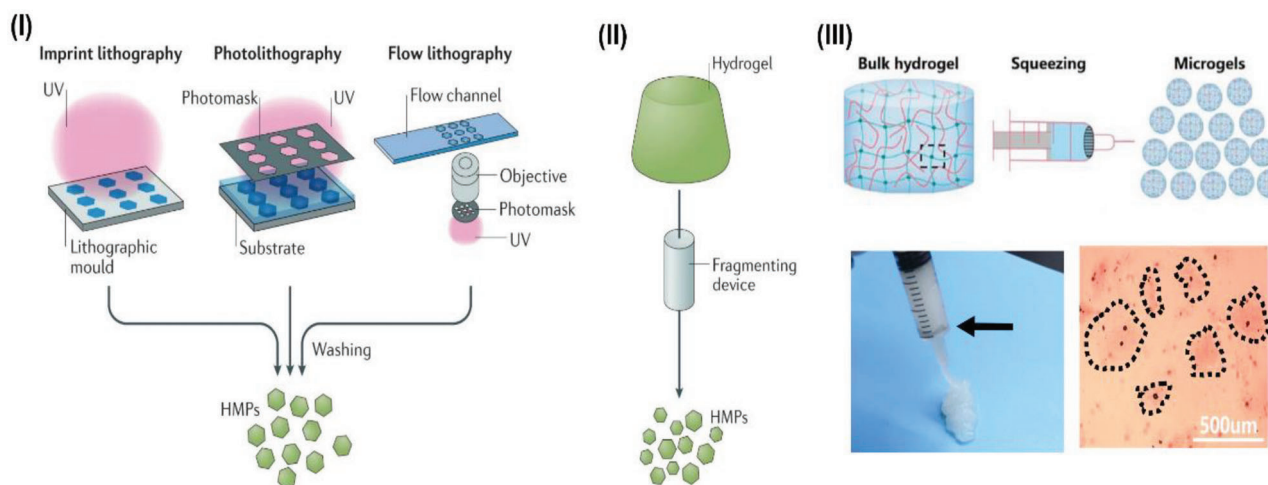


Figure 3. Nonmicrofluidic-based fabrication methods of non-spherical microgels. I) Lithographic methods, including imprint lithography, photolithography, and flow lithography. II) Mechanical fragment method for producing microstrand gels. I,II) Reproduced with permission.^[25b] Copyright 2019, Springer Nature. III) Mechanical fragment method for producing microparticulate gels. Reproduced with permission.^[18] Copyright, 2021 Wiley-VCH GmbH.

3D microchannels are double-sided imprinted in a single elastomer piece that has 1000 parallel flow-focusing generators to enable the parallelization of droplet production. With this 3D MED, droplet generation can be achieved at a rate of $\geq 1000 \text{ mL h}^{-1}$ with 1000 flow-focusing generators on a $6 \times 5 \text{ cm}^2$ device with only one set of inlets and outlets. Based on this design idea, Mealy et al. developed a novel parallelized step emulsification device to provide high throughput microgel generation, as shown in Figure 2IV.^[26b] Briefly, hundreds of identical channels in the device intersect at a taller reservoir channel containing an oil phase. When the aqueous phase flows through the channels to the reservoir channel, macromer droplets containing a crosslinker are formed due to the sudden expansion in channel height at the end of each channel. Then, the droplets can be collected and cured off the chip. This approach can consistently produce microgels for over 12 h in a high-throughput manner, demonstrating one to two orders of magnitude higher production rate than microgels formed using standard and parallelized flow-focusing devices used for similar applications.

In addition, a microfluidic spinning method based on the standard microfluidic technique was developed by Cheng et al. for producing multifunctional hydrogel microfibers with or without loading of cells.^[36] In this method, several injection capillaries are coaxially aligned within a collection capillary. In each injection capillary, a tapered multi-barrel capillary is inserted with several single-barrel capillaries. Then, the hydrogel precursor solution is infused into the injection capillaries while the crosslinking solution is pumped along the same direction into the collection capillary. With this design, a 3D coaxial sheath flow stream forms around the flow of the precursor solution because of hydrodynamic focusing effects. Crosslinking occurs when the two flows meet at the merging point, allowing hydrogel microfibers to be generated in situ. If the precursor solution can flow at a low Reynolds number to form a laminar flow in the microfluidic channels, enabling crosslinking to occur by slow diffusion, the heterogeneous structures and active distributions in the injection flows can be maintained in the obtained hydrogel microfibers.

Thus, the morphology and structure of the microfiber gels can be tightly controlled by the configuration of the injection capillaries.

2.1.2. Stereolithography Techniques

Stereolithography methods, including imprint lithography, photolithography, and flow lithography, have been used as alternative techniques to prepare non-spherical microgels.^[25b,33b] These methods use templated molds and photomasks to control microgel geometry. For imprint lithography, a hydrogel precursor solution is loaded into a templated mold with the negative features of the desired microgels, and the solution is then crosslinked and cured within the mold to obtain microgels with certain features (Figure 3I-left). Similarly, a templated photomask can be used to cover a hydrogel precursor solution when photocrosslinking is applied. Thus, the area not covered by the photomask is crosslinked into microgels while the covered area is not crosslinked. Microgels are collected after removing the non-crosslinked hydrogel precursor (Figure 3I-middle). As imprint lithography and photolithography can only produce microgels in batches, flow lithography has been developed to increase yield through continuous production of microgels.^[25b] As shown in Figure 3I-right, a hydrogel precursor solution flows through a channel where photomasks are used to cure regions of the precursor solution at regular intervals to form microgels. The geometry of the microgels produced by photolithography and flow lithography is determined by the photomask used to cure the hydrogel precursor solution.

2.1.3. Mechanical Fragment Method

Mechanical fragment method, as the name suggests, uses mechanical force to deconstruct bulk nanoporous hydrogels into hydrogel microparticles (HMPs) through a sieve or a grid, as shown

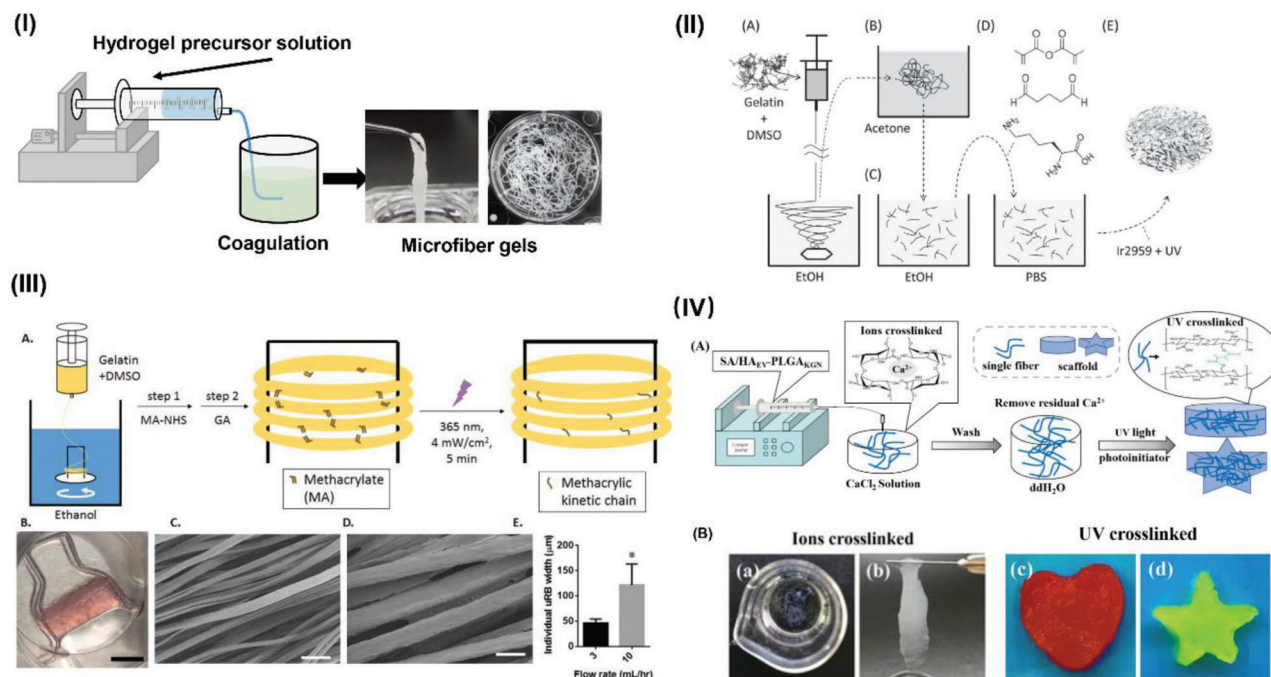


Figure 4. Wet spinning technique for producing non-spherical microgels with high-aspect ratio. I) The schematic illustration of using wet spinning technique to produce microfiber gels. II) Wet spinning was used to fabricate gelatin microribbon gels. Reproduced with permission.^[24a] Copyright, 2013 Wiley-VCH. III) A modified wet spinning technique was used to fabricate aligned gelatin microribbons. Reproduced with permission.^[24c] Copyright 2016, Wiley-VCH GmbH. IV) A modified wet spinning technique was used to produce SA/MeHA microfiber gels for fabricating microporous hydrogels. Reproduced with permission.^[20] Copyright, 2022, Wiley-VCH GmbH.

in Figure 3II. For example, our previous study used a steel sieve to mechanically extrude bulk hydrogel into microparticulate gels with irregular shape (Figure 3III).^[18] In this study, methacrylated hyaluronic acid (MeHA) and 3-aminophenylboronic acid-modified sodium alginate (SABA) nanoporous hydrogels were prepared by exposing the mixture of MeHA, SABA, and bioglass (BG) water suspension to UV light at 365 nm for 30 s. Then, the nanoporous MeHA-SABA bulk hydrogels were squeezed through steel meshes to obtain the MeHA-SABA microgels. The black arrow in the lower-left image of Figure 3III shows the grid inserted in the syringe, and the area marked with dotted lines in the low-right image of Figure 3III is microparticulate gels.

2.2. Techniques for Fabricating Non-spherical Microgels with High Aspect-Ratio

2.2.1. Wet Spinning Technique

Wet spinning is used to produce fibers in industry by extruding a polymer solution through a spinneret into a nonsolvent mixture (coagulant),^[37] as illustrated in Figure 4I. This method can be used to produce microfiber gels. Briefly, a hydrogel precursor solution is prepared by dissolving hydrogel raw materials in a certain solvent. Then, the precursor solution is loaded into a syringe and extruded by a pump through a needle attached to the syringe, into a solution bath containing crosslinkers to the hydrogel precursor. The crosslinking of hydrogel precursor solution results in the formation of hydrogel microfibers. Two strate-

gies have been used to place the needle: one places the needle tip in the crosslinking bath solution, while another places the needle tip over the surface of the crosslinking bath solution. In wet spinning, the size and morphology of resulting microfiber gels are significantly affected by the flow rate and inherent properties of the hydrogel precursor solution, as well as the needle gauge size and concentration of crosslinkers. Optimization of these parameters can effectively prevent needle blockage during injection. Moreover, when non-spherical microgels are used as bio-ink to 3D print macroporous hydrogels, they do not cause blockage due to their shear-thinning rheological properties.

Wet spinning is shown to be a simple, convenient, and controllable method for producing high-aspect-ratio microfiber gels, since it requires no specific equipment or experiment conditions, and the geometry of the microfiber gels can be well controlled.^[15a,16a,c,20,24a,c,38] Han et al. were the first to establish a wet spinning strategy in 2013 to fabricate microribbon-like microgels, as shown in Figure 4II.^[24a] In this study, type-A gelatin microribbons were prepared by ejecting gelatin/dimethyl sulfoxide solution using a pump at room temperature into a tank of anhydrous ethanol (EtOH) (Figure 3II-A). The stream of gelatin was dried in the ethanol into a cluster of microfibers which were further dried in acetone to obtain the gelatin microribbons (Figure 3II-B). To fabricate microporous hydrogels, these as-formed gelatin microribbons were further treated. The post-treatment included microribbon dissociation and washing with ethanol (Figure 4II-C), methacrylation with methacrylic anhydride, fixation with 0.1% glutaraldehyde, washing with deionized (DI) water, and neutralization with L-lysine hydrochloride

in phosphate-buffered saline (PBS) (Figure 4II-D). Then, the post-treated gelatin microribbons were UV crosslinked to form microporous hydrogels (Figure 4II-E). However, this fabrication method is complicated as the microgels needed to be post-treated before they can be used to form bulk hydrogels, and the post-treatments involved several chemicals. Although several wash steps were used to remove the remaining chemicals, there are still concerns about the biocompatibility of the as obtained microgels. In 2016, Lee et al. in the same group used a similar method to fabricate aligned gelatin-based microribbons (μ RBs) by adding a rotating magnet-containing U-shaped collector (750 rpm) in the bottom of the ethanol bath to induce alignment of the as-formed microfibrils, as shown in Figure 4III-A.^[24c] The as-formed microfibrils were then transferred into acetone and flattened into μ RB. Internal crosslinking between μ RBs was performed using aldehyde to maintain the μ RB shape. The collected μ RBs were used to culture smooth muscle cells (SMCs), as shown in Figure 4III-B, and the width of the aligned μ RBs was tunable by varying the ejection rate of gelatin solution during the wet spinning process (Figure 4III-C,D).

Recently, our group established an improved strategy for producing microfiber gels using wet spinning technology without needing any post-treatments of the microfiber gels.^[20] As shown in Figure 4IV-A, we used wet spinning to eject a composite material solution containing SA, MeHA macromolecules, and the photoinitiator lithium phenyl-2,4,6-trimethylbenzoylphosphinate (LAP) into a calcium chloride (CaCl_2) coagulation bath. After the ejected hydrogel precursor fibers arrived in the coagulation bath, the SA macromolecules within the composite precursor fibers were crosslinked immediately, giving rise to partially crosslinked microfiber gels. These microfiber gels were collected, dried by swiping their surface using tissue, and free-stacked in a mold. As the MeHA macromolecules in the partially crosslinked microfiber gels can be further crosslinked in the presence of the photoinitiator LAP and UV light, these as-obtained microfiber gels can be directly used to fabricate microporous gels without needing any post-treatment. This method has distinct advantages compared to existing techniques. First, it has broad application potential due to compatibility with any binary material system, where the two different materials can be crosslinked by different methods and no further chemicals need to be used in the fabrication process. Second, this method allows the encapsulation of bioactive substances within the microfiber gels from the beginning, since no post-treatments involving chemicals are required for the as-obtained microfiber gels. Bioactive substances such as growth factors and extracellular vesicles can be easily encapsulated within the fiber by adding them into the starting composite solution. Figure 4IV-B shows the formation of microfiber gels in the CaCl_2 coagulation bath Figure 4IV-B-a, the yarn of the microfiber gels Figure 4IV-B-b, and the molding of the microfiber gels into differently shaped hydrogels through UV exposure Figure 4IV-B-c,d.

2.2.2. Mechanical Fragment Method

Although the mechanical fragment method has been mainly used to produce non-spherical microgels with low-aspect-ratio,

such as microparticulate gels, Kessel et al. recently used it to produce microstrand gels.^[25c] As shown in Figure 5I, a bulk nanoporous hydrogel was pressed through a grid with micron-sized apertures to form individual entangled microstrands. This method has the advantages of being fast, widely applicable, and scalable, while not requiring specialized equipment. The study demonstrated that the entangled microstrands conferred the characteristics of cell-supporting scaffolds, featuring an interconnected porous network formed from the void spaces between strands and long-term stability in an aqueous solution. The microstrands can also be used for fabricating microporous hydrogels with molding and secondary crosslinking. In addition, they have great application potential as bioinks in 3D bioprinting due to their suitable rheological properties, as well as the ability to align the microstrands during extrusion printing (Figure 5II). Moreover, the printed hydrogel constructs have high fidelity and stable mechanical properties due to the entangled microstrands. The study also showed that cells can be incorporated within the microporous hydrogels through one of two ways, either by inclusion in the bulk gel before deconstruction with the grid or by addition to the entangled microstrands during printing (Figure 5III). Both methods can maintain high viability of the incorporated cells. However, compared to the wet spinning technique, the mechanical fragment method cannot produce the microstrands in a continuous manner, and a bulk hydrogel needs to be fabricated first. In addition, most of the properties of the microstrands are determined by the properties of the starting nanoporous hydrogels and cannot be easily adjusted.

2.3. Features of Different Techniques for Fabricating Non-spherical Microgels

Techniques used to produce non-spherical microgels have different features, which can be selected according to the availability of lab equipment, the properties of raw materials, and the applications of the microgels. The key performance metrics of different techniques for fabricating non-spherical microgels are listed in Table 4. Microfluidic and lithography techniques need specific equipment and microfabrication technologies, while mechanical fragment and wet spinning techniques are simple and do not require advanced equipment and technologies. Both microfluidic and wet spinning techniques can continuously produce microgels while the mechanical fragment methods can only produce microgels in a batch-to-batch manner. Among lithographic methods, imprint lithography and photolithography can only produce microgels batch-to-batch while flow lithography can produce microgels in a continuous mode.

The microfluidic, lithography, and wet spinning techniques have advantages in controlling the geometry of microgels and producing monodisperse microgels over the mechanical fragment method. The geometry of the microchannels on the chip used in the microfluidic technique can control the final geometry of the microgels. The polydispersity of polymerized microgels or particles can reach 1.5, which is similar to that of spherical microgels produced by microfluidic emulsion technology. The microgels with disk shape can have diameter distribution in the range of 102–106 μm , while microrods can have length distribution in the range of 820–860 μm .^[33a] Meanwhile, the

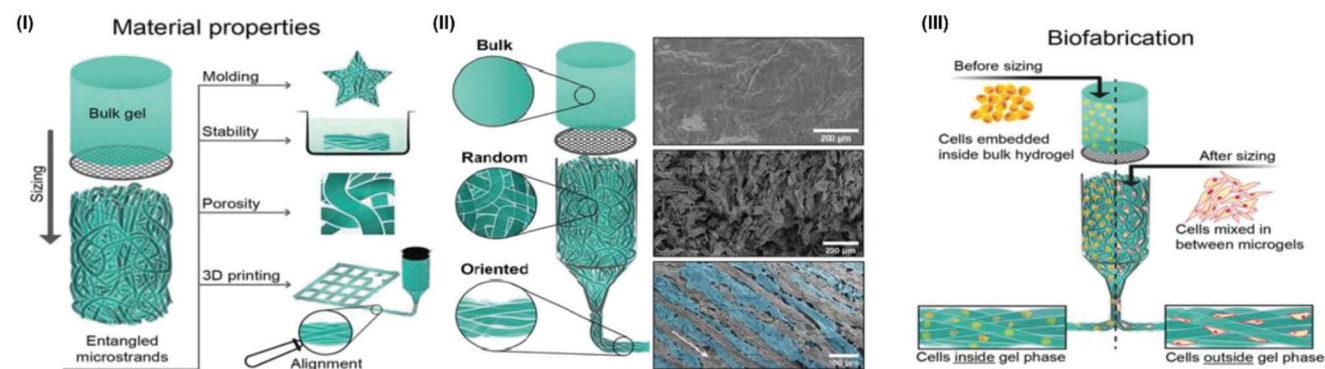


Figure 5. I) Bulk hydrogel is mechanically extruded through a grid to deconstruct it into microstrands. II) The microstrands are moldable, stable in aqueous solutions, porous, printable and can be aligned by extrusion. III) A bioink can be created based on these microstrands. Reproduced under the terms of the Creative Commons CC-BY license.^[25c] Copyright 2020, The Authors, published by Wiley-VCH GmbH.

geometrical features of the masks or molds used in lithography technologies can precisely control the geometry and monodispersity of the resulting microgels.^[30a,33b] More importantly, the molds and masks used in lithography and the microchannels used in microfluidic techniques allow easy adjustment of nanoscale features, enabling the generation of microgels with tailored internal and external architectures that cannot be achieved with other fabrication methods.^[39] Different from microfluidic and lithography techniques, wet spinning tightly controls the geometry of microgels by adjusting the processing and material parameters, such as flow rate, needle size, concentration of hydrogel precursor solution, and concentration of crosslinkers.^[40] The shape of the wet-spun microgel is usually microfibers with a round cross-section. By post-treating the obtained microfibers, such as through drying, microribbons with a flat cross-section can be obtained.^[15a,16c,24a] The geometry of microgels produced by the mechanical fragment method is determined by the pores of the tools used to break the bulk nanoporous hydrogels, which may be in the shape of microparticulates and microstrands.^[18,25c]

Regarding the application limits of each technique, low-viscosity hydrogel precursor solutions and oil are necessary for producing non-spherical microgels using the microfluidic technique, while no oil or surfactants are required for lithography. A proper crosslinker to the hydrogel precursor solution is required for producing microgels with wet spinning. In addition, the viscosity of the hydrogel precursor solution should be compatible

with the flow rate of the perfusion pump and the gauge size of the needles used for producing microgels. A high flow rate of the hydrogel solution is usually used in wet spinning since this can result in smaller diameter of the microfiber gels. For example, when the needle tip is placed under the surface of a calcium chloride coagulation bath solution, to form SA microfibers with diameter smaller than 500 μm , the minimum flow rate of the SA solution with 2% concentration is about 10 mL min^{-1} to avoid aggregates or bubbles.^[20] The needle tip can also be placed over the surface of the crosslinking solution and allow a lower flow rate to be used. For example, when the needle tip was placed at a height of 1.8 m over the surface of an ethanol solution when a gelatin solution was ejected using a syringe pump, the flow rate of the extruded solution could be set to 5 mL h^{-1} .^[15a]

3. Progress in the Fabrication of Microporous Hydrogels from Non-spherical Microgels

3.1. The Development History of Microporous Hydrogels Made from Non-spherical Microgels

The first application of microgels in tissue engineering and regenerative medicine (TERM) was for studying cell/material interactions by encapsulating cells within the microgels, which avoided diffusion limitations of nutrients and wastes and facilitated analysis techniques of single or collective cells.^[41] Up

Table 4. Key performance metrics of different techniques for producing non-spherical microgels.

Production Methods	Control of the microgel geometry	Production rate	Specific equipment required	Use of oils	Cell compatibility	Geometry of the microgels
Microfluidic methods ^[16b,41]	High	Average	Yes	Yes	Average (>80% viability)	Microrods
Lithographic methods ^[33b,42]	High	Average	Yes	Yes	Average (>80% viability)	Polygon Microrods
Mechanical fragment methods ^[18,25c]	Low	Average	No	No	Average (>80% viability)	Microrods Microparticulate
Wet spinning methods ^[16c,20,24a]	High	High	No	No	Average (>80% viability)	Microfibers Microribbons

until 2013, this application was limited to spherical microgels, as there were no methods available to produce monodisperse, anisometric soft microgels for studying cells inside an anisometric architecture. When non-spherical microgels were developed, their first application was in loading cells for studying cell/material interactions^[43] In 2013, meter-long cell-laden hydrogel microfibers were first produced to artificially reconstruct fiber-shaped cellular constructs by encapsulating ECM proteins and differentiated cells or somatic stem cells. It was suggested that the cellular constructs could be used as templates to reconstruct fiber-shaped functional tissues that mimic muscle fibers, blood vessels, or nerve networks.^[43] In 2019, Guerzoni et al. used a radical-free microfluidic system to produce monodisperse, anisometric poly(ethylene) glycol (PEG) microgels to study the effects of the fibers on the behavior of cells inside an anisometric architecture. These microgels were found to potentially direct cell growth and could be injected as rod-shaped minitissues, which further assembled into organized macroscopic and microporous structures post-injection. Their aspect-ratio could be adjusted with flow parameters, while mechanical and biochemical properties were controlled by modifying the precursors. Encapsulated primary fibroblasts were viable and showed spreading and migration across the 3D microgel structure, demonstrating the potential application of these microgels in TERM^[41]

Based on the above findings of applying non-spherical microgels in studies of cell/material interactions and artificial construct development, as well as the emergence of microgel assembly fabrication methods, the use of non-spherical microgels in fabricating microporous injectable hydrogels began in 2013. A recent 2022 review has comprehensively discussed microporous injectable hydrogels made of spherical or low-aspect-ratio microgels using the microgel assembly method.^[14b] In comparison to those made from spherical microgels, microporous injectable hydrogels fabricated from non-spherical, particularly high-aspect-ratio microgels, have increased pore size, enhanced porosity, high mechanical stability, and improved specific anisotropy.^[7b,15a,16c,17,22d,24a,c,38b] In addition, unlike hydrogels comprising spherical microgels, those made from non-spherical microgels have the unique ability to guide cell alignment and polarization and stimulate the formation of tissue with a highly hierarchical structure.^[24c] Since 2013, hydrogels prepared from wet-spun microribbon-like microgels have been used for various applications in tissue regeneration and attracted increasing attention.^[15a,16c,34,38,44] Some of the hydrogels with anisotropic structures have shown advantages in prompting the growth of certain tissues such as articular cartilage.^[15a,16c] Since the majority of human tissues have highly hierarchical structures, microporous hydrogel scaffolds made of non-spherical microgels have higher application potential than those made of spherical microgels. In the following sections, we concentrate on discussing the fabrication techniques and TERM applications of microporous hydrogels comprising non-spherical microgels.

3.2. Microporous Hydrogels Comprising Non-spherical Microgels Produced by Mechanical Fragment Method

Microporous hydrogels comprising non-spherical microgels have been fabricated by the mechanical fragment method. Kessel

et al. produced iota-carrageenan entangled microstrands by pressing an iota-carrageenan bulk nanoporous hydrogel through a grid.^[25c] The microstrands were then used as bioinks to fabricate large, complex, and microporous hydrogel constructs. As shown in **Figure 6I**, a 3D-model (Figure 6I-A) and the printing path (Figure 6I-B) were first created by the slicing software, followed by printing of a macro-sized (28 × 14 × 7 mm) ear-shaped structure with entangled microstrands (Figure 6I-C). The printed constructs had clear and visible individual layers and deposited filaments, which clearly reproduced the designed printing path (Figure 6I-C). These printed structures were reported to have long-term fidelity and high mechanical stability as the whole structure kept stable even after 15 layers. The study demonstrated that the entangled microstrands exhibited all relevant rheological properties necessary for extrusion 3D bioprinting, such as shear thinning behavior and shear recovery, indicating the good injectability of the microstrands. The resulting printed microporous hydrogels had aligned microstrands in the direction of printing, while the bulk hydrogels possessed randomly entangled microstrands. Thus, anisotropic structures could be successfully formed by orienting the alignment of microstrands through the printing process.

Recently, our group used a mechanical fragment method to produce irregular non-spherical microgels according to the procedures described in our previous study.^[18] Briefly, MeHA and boric acid-modified sodium alginate (BASA) were used to fabricate nanoporous MeHA-BASA hydrogels, which were squeezed through a steel mesh to form irregular microparticulate microgels. Then, these MeHA-SABA microgels were mixed with bio-glass (BG) water suspension, during which Ca²⁺ and OH⁻ ions were released from BG. The released OH⁻ ions created an alkaline environment to induce the formation of dynamic B–O bonds, while the Ca²⁺ ions induced the assembly of MeHA-SABA microgels by SA in the microgels. Microporous hydrogels were successfully fabricated through the formation of voids between the microgels, with pore sizes that were significantly larger than nanoporous hydrogels (Figure 6II). Additionally, these microporous hydrogels had good self-healing properties due to the formation of dynamic B–O bonds and could release bioactive BG ions that provide chemical cues to modulate cell behavior. By varying the content of BG in the material system, the gelation behavior of the hydrogels can be adjusted to obtain injectable MeHA-SABA microporous hydrogels. The study showed that the microporous hydrogel could be injected into different molds to fill various complex shapes. The irregular microparticulate squeezed through the mesh resulted in polygonal pores within the hydrogels.

3.3. Microporous Hydrogels Comprising Non-spherical Microgels Produced by Wet Spinning

Wet spinning technology has been widely used to produce microribbons from different types of materials. In 2013, Han et al. first used wet spinning to produce microribbon-like microgels and used these to fabricate microporous hydrogels.^[24a] According to the method described in Figure 4II, the gelatin microfiber gels were ejected from a syringe needle fed by a syringe pump. The properties of the microribbons could be adjusted by varying

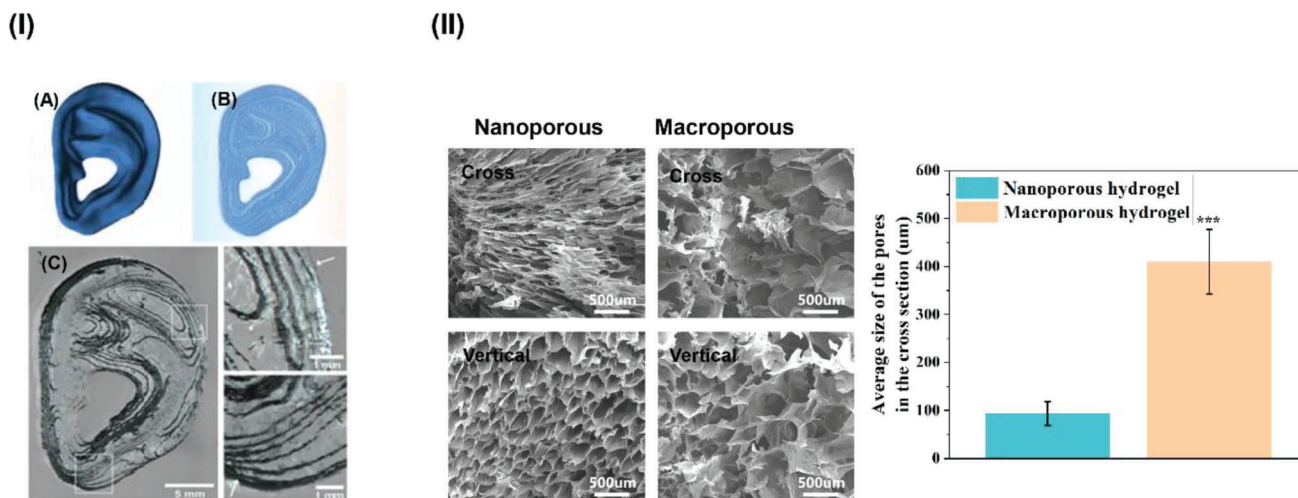


Figure 6. Microporous hydrogels made from non-spherical microgels fabricated by mechanical fragment methods. I) A macro-sized ear-shaped hydrogel construct was printed with the microstrands obtained by squeezing nanoporous hydrogels through a grid with apertures. Reproduced under the terms of the Creative Commons CC-BY license.^[25c] Copyright 2020, The Authors, published by Wiley-VCH GmbH. II) The microporous hydrogels have larger pores than the nanoporous hydrogels. Reproduced with permission.^[18] Copyright 2021, Elsevier.

the wet spinning rate, drying temperature, drying agent, and level of glutaraldehyde crosslinking while the hydrogel properties depended on the morphology of microribbons and the microribbon density. Wider microribbons were obtained when the flow rate was increased. For example, when the solution was pumped at a flow rate of 5 mL h^{-1} , the average width of the microribbons was $40 \mu\text{m}$ with a range of $20\text{--}50 \mu\text{m}$ (Figure 7I-A–C). When the flow rate was increased to 10 mL h^{-1} , the average microribbon width became $70 \mu\text{m}$ with a range of $60\text{--}90 \mu\text{m}$ (Figure 7I-D–F). After exposure to UV light, the microribbons fused into a scaffold with interconnected microporous channels from the voids formed between microribbons, providing a microporous scaffold structure that offered ample space for nutrient diffusion, cell proliferation, and matrix production. Since the microribbons were flat and had high-aspect-ratio, they had the appearance of a “highway”, and the scaffold resembled a “highway system.” The density of microribbons significantly affected the porosity of the microporous hydrogels, as a higher density led to increased fusion between neighboring microribbons. As shown in Figure 7I, the diameter of interconnected scaffold pores was inversely related to the density of microribbons. When the microporous scaffolds were made of microribbons with the same width ($40 \mu\text{m}$ or $70 \mu\text{m}$), increasing the density of microribbons from 2.5 to 10% (w/v) led to a decrease in pore size from 250 to $50 \mu\text{m}$. Thus, while increasing microribbon density provides more internal surface area to support cell proliferation, it also reduces the microporosity of the scaffold. Additionally, the study noted volume shrinkage of the scaffolds during photocrosslinking, where the shrinkage degree was slightly dependent on microribbon density but was not affected by other fabrication parameters such as feeding rate, degree of aldehyde fixation, or drying temperature. Following photocrosslinking, the scaffolds remained geometrically stable in PBS at 37°C , and almost no swelling was observed. The microporous hydrogels comprising these flat and high-aspect-ratio microribbons showed a very good anisotropic structure. However, hydrogel injectability was impaired as several post-ejection

treatments were required for obtaining microribbons with a certain width.

Recently, our group used wet spinning to produce SA/MeHA microfiber gels and assembled these into microporous hydrogels by further crosslinking the gels to each other using UV irradiation in the presence of the photoinitiator LAP,^[20] as illustrated in Figure 4IV-A. The SA/MeHA microfibers could be injected into different molds and formed microporous hydrogels replicating the shape of the mold once exposed to UV light. Based on this method, microporous hydrogels were obtained as shown in Figure 7II. It can be seen from the optical images that large microscale pores were present on the surface and interior of the wet hydrogels (μ -fiber scaffold) (Figure 7II-a1,b1), indicated by arrows). However, these pores could not be found in the traditional nanoporous hydrogels (HG) (Figure 7IIa,b). When the hydrogels were freeze-dried and observed with scanning electronic microscopy (SEM), large spaces were apparent between thick and high-aspect-ratio microfibers in the hydrogel cross-section (Figure 7II-c1), indicated by arrows). These spaces were long and narrow gaps that existed between microfibers, resulting in a clear anisotropic structure within the microporous hydrogel. In addition, the degradation rate of the microporous μ -fiber hydrogel was faster than the HG when immersed in simulated body fluid (SBF). As shown in Figure 7III, after 21 d of incubation in SBF, the original cylinder shape of microporous μ -fiber hydrogel started to change and μ -fibers departed from the scaffolds into SBF, while the HG maintained its shape. The microporous μ -fiber hydrogels also showed significantly improved stability under cyclic compression compared to HG due to their great shock-absorbing capacity. As shown in Figure 7IV, when the two types of hydrogel scaffolds were both subjected to cyclic compression, the structure of HG was easily damaged, and the scaffold failed to return to its original shape after the first compression with 50% strain. Thus, no further compression could be performed on the HG. Remarkably, the microporous μ -fiber hydrogel maintained its structure well during cyclic

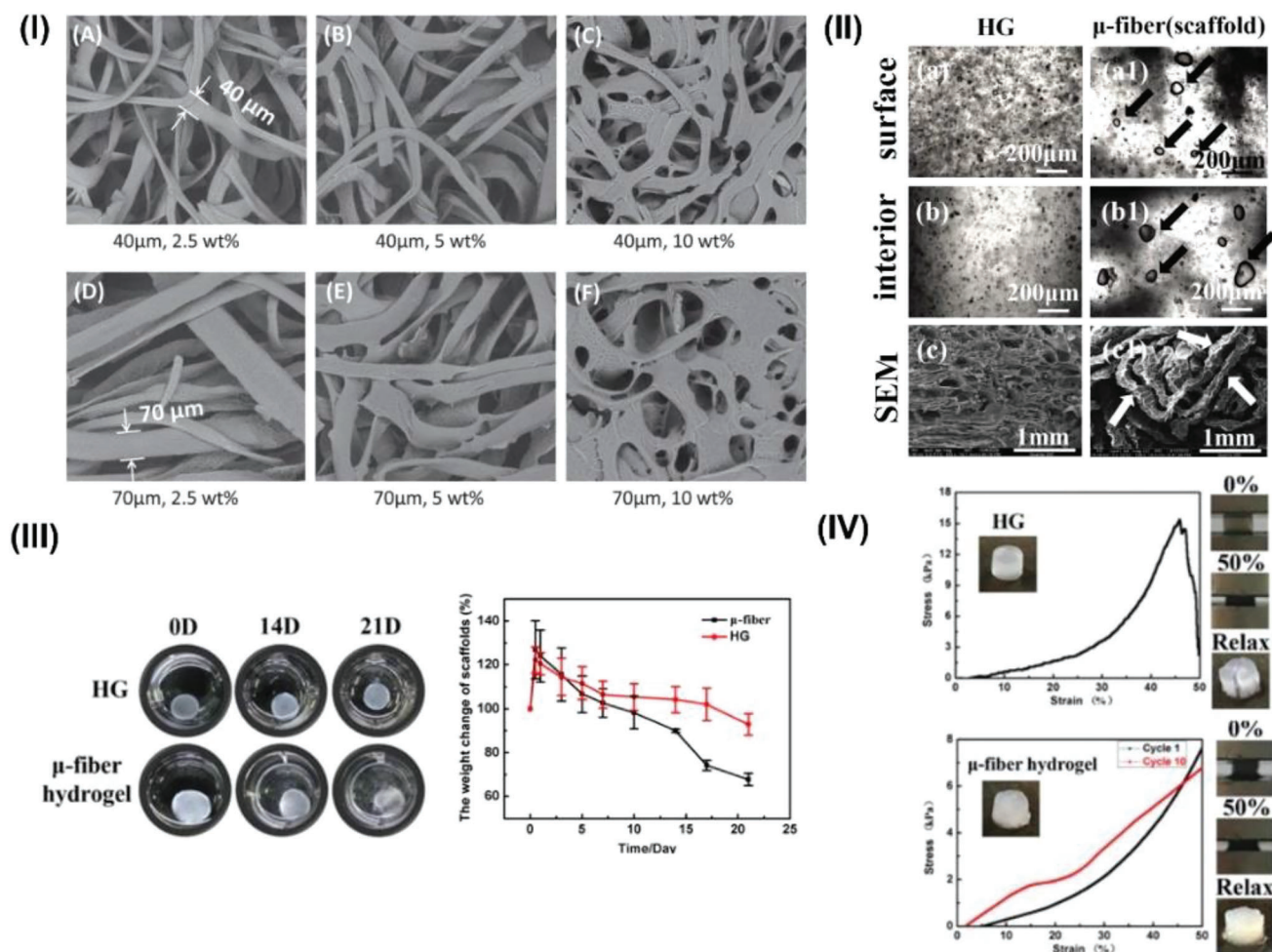


Figure 7. Microporous hydrogels made from non-spherical microgels fabricated by wet spinning technology. I) Microporous hydrogels were fabricated by assembling microribbon gels. Reproduced with permission.^[24a] Copyright 2013, Wiley-VCH GmbH. II) Microporous μ-fiber hydrogels (μ-fiber scaffold) fabricated by assembling microfiber gels had obviously larger spaces between the microfibers than traditional nanoporous hydrogels (HG). III) The μ-fiber hydrogel degraded faster than HG in SBF. IV) The μ-fiber hydrogel had excellent shock-absorbance capability to maintain its structural stability. II–IV) Reproduced with permission.^[20] Copyright 2022, Wiley-VCH GmbH.

compression and could successfully recover to its original shape after removing the external force. The hydrogels maintained a similar stress-strain curve even after ten compression cycles, indicating excellent shock-absorbance capability (Figure 7IV). Our study suggested that bioactive substances, such as small extracellular vesicles and microspheres containing drugs, could be incorporated into the SA/MeHA microfiber gels to improve the bioactivity of the bulk composite hydrogel. Thus, the microporous μ-fiber hydrogels have wide application potential for tissue regeneration with their microporous structure, improved mechanical properties, and tunable bioactivity.

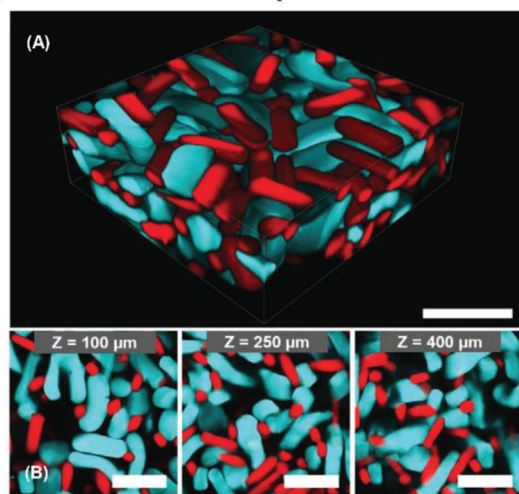
3.4. Microporous Hydrogels Comprising Non-spherical Microgels Produced by Other Methods

Other methods for producing non-spherical microgels include microcontact printing, microfluidics, and in-mold polymerization techniques. For example, poly(lactide-co-glycolide) (PLGA)

microribbons made by microcontact printing have been used to fabricate microporous hydrogels. These microribbons were post-coated with fibrinogen to enhance their solubility and injectability, followed by mixing with thrombin to inter-crosslink into 3D scaffolds.^[34] Two recent studies have produced rod-shaped microgels with microfluidics techniques and used these to fabricate microporous scaffolds.^[17,22d] The microgels were injectable and could be further crosslinked to form larger injectable hydrogels with anisotropic microporous structures. In the first study, microfluidic droplet generators were used to produce spherical and rod-shaped microgels with photo-crosslinkable norbornene-modified hyaluronic acid. These microgels were then formed into shear-thinning and self-healing granular hydrogels.^[17]

In the second study, rod-shaped microgels were produced by plug-flow microfluidics and photoinitiated free-radical polymerization of eight-arm star-PEG-acrylate (sPEG-AC).^[22d] After the formation of the microgels, they were functionalized with either reactive epoxy groups or primary amines during polymerization on-chip by the respective addition of glycidyl methacrylate

(I) Interlinked Macroporous Scaffold



(II)

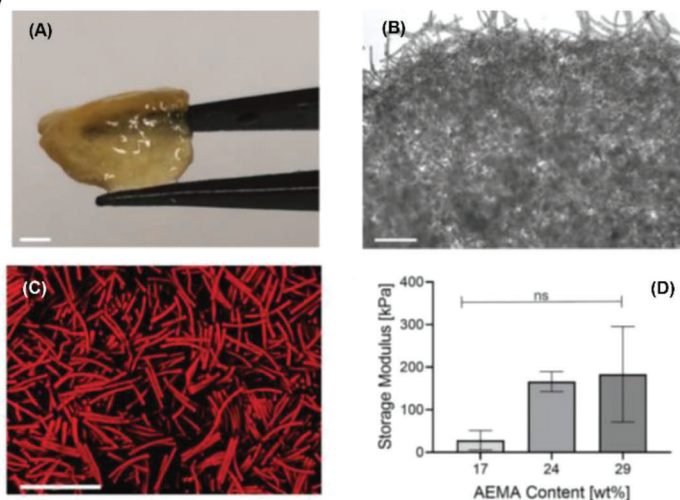


Figure 8. Microporous hydrogels made from non-spherical microgels fabricated by microfluidics and in-mold polymerization. I) Microporous hydrogels were fabricated by interlink rod-shape microgels produced by microfluidics. Scale bar represents 500 μm . Reproduced under the terms of the Creative Commons CC-BY license.^[22d] Copyright 2022, The Authors, published by Wiley-VCH GmbH. II) Rod-shape microgels produced with in-mold polymerization were assembled into microporous hydrogels, and the storage modulus of the hydrogels can be adjusted by changing the AEMA content. Reproduced under the terms of the Creative Commons CC-BY license.^[7b] Copyright 2022, The Authors, published by Wiley-VCH GmbH.

(GMA) or 2-aminoethyl methacrylate (AMA) comonomers. As the microgels had complementary reactive groups, an amine-epoxy addition reaction was then performed by mixing under aqueous conditions without requiring any other reagents to interlink the microgels into 3D microporous scaffolds. **Figure 8I-A** shows the interlinked microgel rod-based scaffold made from epoxy-functionalized microgel rods (7.90 mg mL^{-1} GMA, 10 wt% sPEG-AC, red methacryloxyethyl thiocarbonyl rhodamine-B) mixed with the same number of amine-functionalized microgel rods (12.15 mg mL^{-1} AMA, 10 wt% sPEG-AC, cyan FITC). The interlinked scaffold had a porous structure, observed with confocal microscopy at different Z-values (indicated in the insertion) as shown in **Figure 8I-B**. The pore sizes of these microporous hydrogels built with rod-shaped microgels were about 4.5-fold larger compared to similar scaffolds made from spherical microgels. In addition, the microporous hydrogels had a highly interconnected pore network with anisotropic tubular-like pore shapes, which could guide the anisotropic behavior of cells in tissue regeneration. Rapid crosslinking also fixated the rod-shaped microgels in their jammed state, not giving them time to form densely packed stacks. Hence, the microporous hydrogels in this study had larger pore sizes compared to hydrogels made from microgels that are not covalently interlinked, and thus might result in a more nematic ordered scaffold.^[22d]

A limitation in microfluidic techniques is related to down-scaling the reliable microgel size since the microgel diameter is dependent on the channel size. Moreover, it is difficult to guarantee consistency in the properties of microgels due to high batch-to-batch variation in flow rates, temperature, and other environmental conditions during fabrication.^[7b] Therefore, Suterin et al. used an established in-mold polymerization method to produce anisometric microgel building blocks, named particle replication in nonwetting templates (PRINT).^[7b] This study fabricated anisometric, monodisperse microgels by copolymerizing PEG

diacrylate (PEG-DA, 700 g mol^{-1}) and 2-aminoethyl methacrylate (AEMA) using PRINT. Three types of microgels with different aspect-ratios ($10 \times 10 \times 50 \text{ }\mu\text{m}^3$ (aspect-ratio 5), $10 \times 10 \times 100 \text{ }\mu\text{m}^3$ (aspect-ratio 10), and $10 \times 10 \times 200 \text{ }\mu\text{m}^3$ (aspect-ratio 20)) were used to fabricate microporous hydrogels. As shown in **Figure 8II-A**, microporous scaffolds with large size can be easily obtained. For example, 400 000 microgels (1 microgel: $10 \times 10 \times 100 \text{ }\mu\text{m}^3$, total microgel volume: 3.78 mm^3) can be annealed into a large scaffold with a volume of $\approx 400 \text{ mm}^3$ (**Figure 8II-A**). **Figure 8II-B,C** shows the microscopic images of the scaffolds, demonstrating their microporous structure. The scaffolds were shown to withstand strong mechanical stress without fracturing, and their storage modulus was tunable by adjusting the AEMA content **Figure 8II-D**. The advantages and disadvantages of microporous hydrogels comprising non-spherical microgels produced using different methods are summarized in **Table 5**. It should be noted that several factors can impact the final pore structure of the assembled microporous hydrogels, including microgel properties such as geometry, size or aspect-ratio, stiffness, crosslinking condition, and the density of microgels in the hydrogel. **Table 5** only summarizes some general features of the different microporous hydrogels, as it is difficult to quantitatively compare their properties since they comprise non-spherical microgels containing different materials and made using different methods.

4. Applications of Microporous Hydrogels Made of Non-spherical Microgels in Tissue Regeneration

Hydrogels made from spherical microgels cannot provide important guidance cues for aligning cells or regenerating tissues with anisotropic structure, due to their homogeneous structure and close-packed lattice that limits interaction between individual spheres. With the development of microporous hydrogels assembled with non-spherical microgels, especially high-aspect-ratio

Table 5. Key features of microporous hydrogels comprising non-spherical microgels produced using different methods.

Microgel production Methods	Microgel geometry	Microgel aspect-ratio	Hydrogel pore shape	Hydrogel mechanical stability	Hydrogel mechanical flexibility
Microfluidic methods ^[16b,41]	Microrods	Low (1-5)	Short and narrow gaps	High	Moderate
Lithographic methods ^[33b,42]	Polygon	Low (1-5)	Irregular voids	Moderate	Moderate
Mechanical fragment methods ^[18]	Microparticulate	Low (1-5)	Irregular voids	Moderate	Moderate
Mechanical fragment methods ^[25c]	Microstrands	High (>5)	Long and narrow gap	High	High
Wet spinning methods ^[16c,20,24a]	Microfibers Microribbons	High (>5)	Long and narrow gap	High	High
In-mold polymerization ^[7b]	Microrods	High (>5)	Long and narrow gap	High	High

microgels such as microribbons, microstrands, microfibers, and microrods, their applications in anisotropic tissue regeneration have been increasingly explored.^[16a,c,20,24a,c,25c,38] A limited number of studies are currently available in this area, most of which focused on cartilage regeneration.^[15a,16a,c,20,24a,25c,38a] Studies reporting other types of tissue regeneration are rare, including only one on muscle^[24c] and another on bone.^[38b] In this section, we discuss the current applications of microporous hydrogels made of non-spherical microgels in tissue regeneration including cartilage, muscle, and bone regeneration.

4.1. Application of Microporous Hydrogels Made of Non-spherical Microgels in Articular Cartilage Regeneration

4.1.1. Challenges of Existing Articular Cartilage Repair Techniques

Articular cartilage injuries are highly prevalent in all age groups and pose a significant clinical challenge, since long-term repair remains difficult, and injuries often lead to the progression of osteoarthritis or become a cause of chronic disability in a young and otherwise healthy population. Articular cartilage lacks intrinsic tissue healing capacity due to the limited number and mobility of chondrocytes, and lack of access to vascular, neural, and lymphatic networks as well as a source of progenitor cells that could otherwise help with regeneration.^[45] Moreover, repair strategies targeted only at the cartilage layer are often inefficient, since long-term repair and maintenance of articular cartilage relies on integration and support from the underlying intact subchondral bone. Common clinical interventions for cartilage injuries include chondroplasty, microfracture, mosaicplasty, and more modern cartilage regeneration approaches such as autologous chondrocyte implantation (ACI) and matrix-associated ACI (MACI).^[46] However, current clinical treatments face critical challenges and in many cases are unable to sustain long-term repair, due to secondary operations, donor site morbidity, cell loss, formation of mechanically inferior fibrocartilage, long post-operative recovery time, and restriction to a small fraction of the patient population with near-ideal surgical conditions, suggesting the high demand for new strategies in inducing cartilage regeneration.^[47] Articular cartilage tissue engineering has attracted increasing attention in the last decades and various types of scaffolds have been developed, which have been reviewed in recent literature.^[46,48] Injectable hydrogels have been widely

used as matrices for cartilage tissue regeneration given their injectability and ability to fill defects with irregular shapes.^[20] However, traditional nanoporous hydrogels usually restrain the encapsulated cells or impede the infiltration of endogenous cells from subchondral bone into the damaged cartilage layer, which could delay new ECM deposition and the progress of tissue repair. Thus, the development of microporous hydrogels is in pressing demand for accelerating cartilage regeneration.

4.1.2. Microporous Hydrogels for Cartilage Regeneration

Recently, hydrogels assembled with microribbons produced by wet spinning have demonstrated the advantages of anisotropic gels in cartilage tissue engineering.^[15a,16a,c,20,24a] Yang's group was the first to demonstrate the potential of using gelatin-based microporous hydrogels assembled with microribbon gels for cartilage regeneration, after they established the methods to produce microribbon gels using wet spinning and fabricate microporous hydrogels with the microribbons.^[15a,24a,38a] For example, in 2018, Conrad et al. from this research group demonstrated that their gelatin-based microribbon (μ RB) hydrogels could be used as novel 3D matrices for accelerating chondrogenesis and new cartilage formation with improved mechanical properties.^[15a] The μ RB hydrogels were inherently microporous and exhibited cartilage-mimicking shock-absorbing mechanical properties. After MSCs were cultured in μ RB hydrogels for 21 d, the cell-seeded hydrogel constructs exhibited a 20-fold increase in compressive modulus to 225 kPa, approaching the level of native cartilage. In contrast, the MSCs-seeded traditional nanoporous hydrogels only showed a modest increase in compressive modulus to 65 kPa. This significant difference was caused by a substantial increase in the total amount of neocartilage produced by MSCs in the μ RB hydrogels, due to their improved interconnectivity and mechanical strength compared to nanoporous hydrogels.

In 2020, the same group improved the hydrogel design by incorporating degradable nanoporous chondroitin sulfate hydrogel into the gelatin-based μ RB hydrogel to develop a composite microporous hydrogel.^[16c] In addition, the group loaded the composite hydrogel with cocultures of adipose-derived stem cells and neonatal chondrocytes. The study showed that the compressive modulus of the neocartilage produced by the cocultured cells within the composite hydrogel reached \approx 330 kPa, and the quality of the cartilage was better than that produced by neonatal

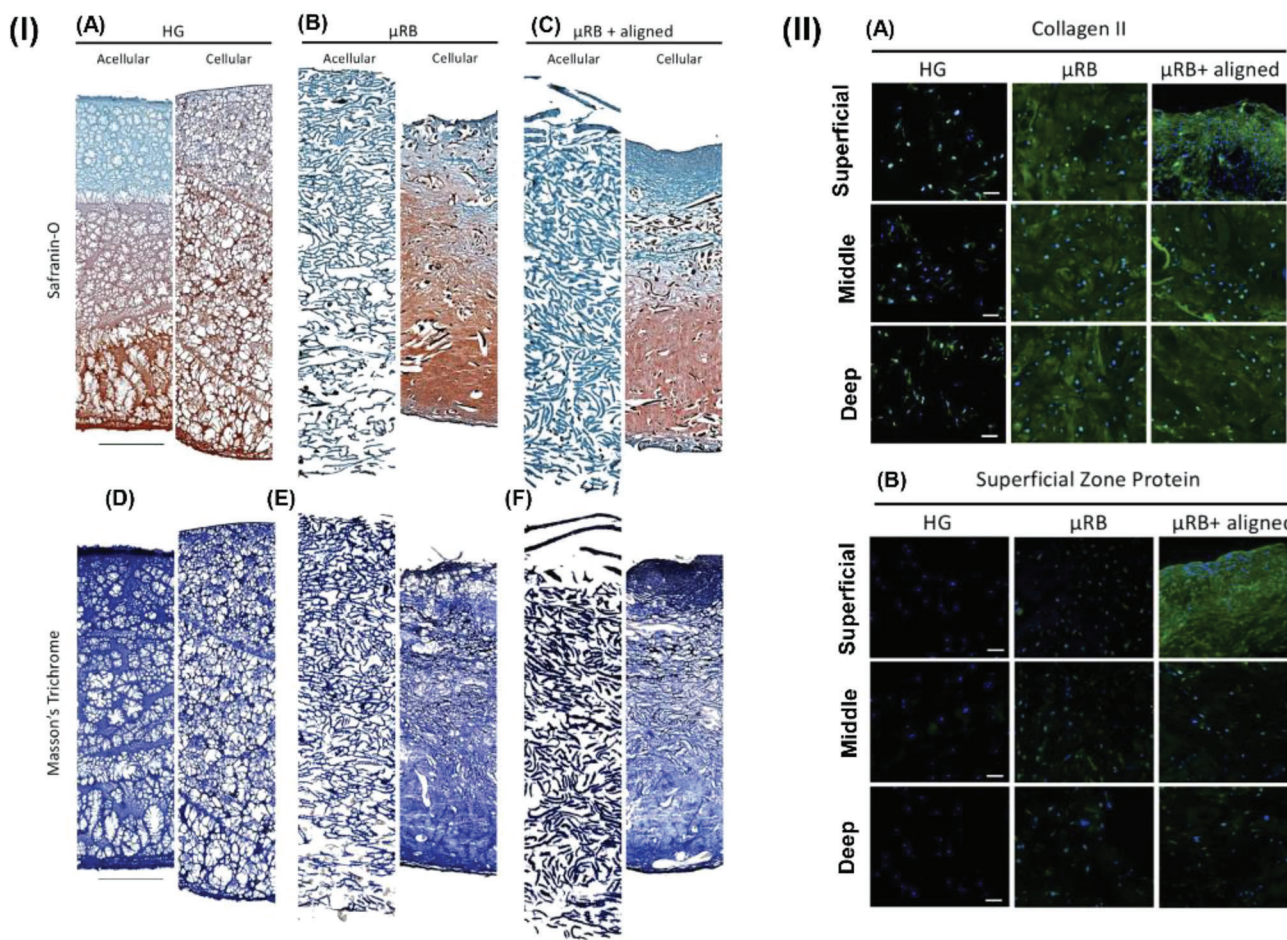


Figure 9. Cartilage formation in microporous hydrogels fabricated with microribbons. I) The μ RB scaffold enhanced GAG and collagen deposition in a zonal manner mimicking articular cartilage structure, in contrast to the tri-layer HG scaffold that showed very little ECM deposition. Scale bars: 1 mm. II) The μ RB scaffolds promoted Collagen II production throughout all zones (A) and superficial zone protein was produced only in superficial zone of the μ RB + aligned scaffold at Day 21 (B). Scale bars: 100 μ m. Reproduced with permission.^[16a] Copyright 2019, Elsevier.

chondrocytes alone. In the same year, Gegg et al. from the same group fabricated trilayer μ RB hydrogels, with or without an additional layer of aligned microribbons to further support robust cartilaginous ECM deposition.^[16a] These trilayer μ RB hydrogels seeded with MSCs were found to induce neocartilage formation with increased compressive modulus of up to 456 kPa, as well as a biomimetic zonal arrangement in the regenerated cartilage with more than fourfold increase in GAG production from the superficial to deep zones. Additionally, the additional layer of aligned gelatin μ RBs in the superficial zone further enhanced biomimicry of the neocartilage, leading to robust collagen deposition and protein production in the superficial zone (Figure 9).

As an alternative strategy for producing microporous hydrogels with anisotropic structure for cartilage regeneration, Kessel et al. obtained microstrand gels by squeezing bulk nanoporous hydrogels through a grid and used 3D bioprinting to make microporous hydrogels from these microstrands.^[25c] By loading cells within the bulk nanoporous hydrogels before squeezing through the grid, the cells could become encapsulated within single microstrands, and their viability was not affected by the squeezing process. To produce constructs for cartilage regeneration, the

study mixed chondrocytes alongside the as-obtained entangled microstrands and used the mixture as bioinks for 3D bioprinting, and the microstrands could become automatically aligned during extrusion, as illustrated in Figure 10I-A. The cell viability remained above 90% after printing and did not change significantly during in vitro culture for 42 d in the bioprinted hydrogels, while the appearance of the hydrogel constructs changed from being translucent at day 0 to white and cartilage-like at day 42, suggesting abundant ECM deposition (Figure 10I-B). In addition, the modulus of the construct significantly increased from 2.7 kPa at day 0 to 212 ± 83.7 kPa at day 21 and finally reached 780.2 ± 218.4 kPa at day 42 (Figure 10I-C). Histological staining indicated that cartilaginous matrix deposited within the hydrogel after 21 and 42 d of culture, and cells were able to migrate into the space previously occupied by the hydrogel microstrands ((Figure 10I-D)). This study was the first to explore the application of entangled microstrand gels as a bioink for 3D bioprinting, as well as to combine these microgels using 3D bioprinting to produce microporous hydrogels.

The above studies demonstrated the significant advantages of using microporous hydrogels comprising non-spherical

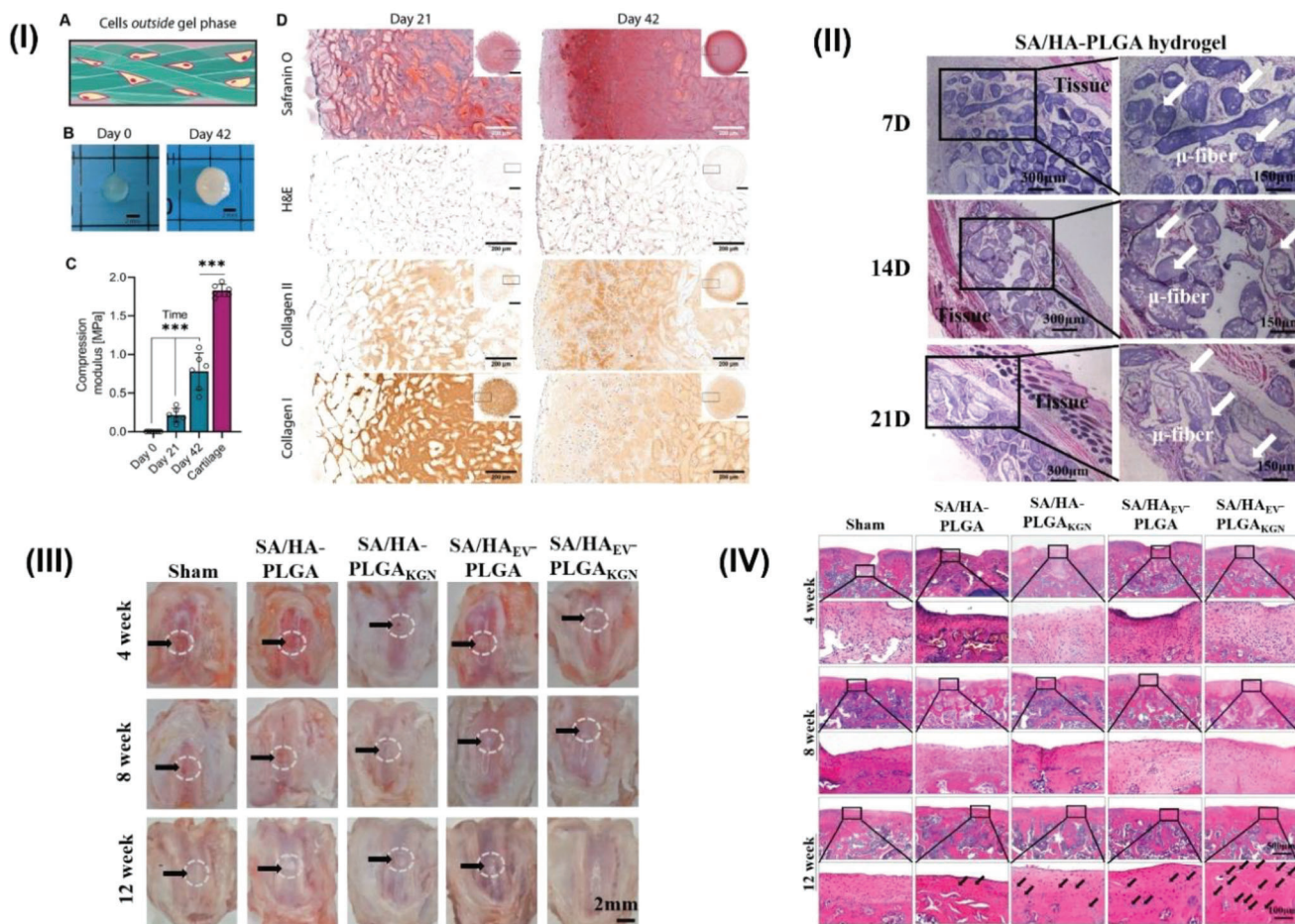


Figure 10. Cartilage formation in microporous hydrogel comprising microstrand gels. I) Bioprinted hydrogel construct with microstrands formed cartilage-like tissue after 42 d of in vitro culture. Reproduced under the terms of the Creative Commons CC BY license.^[25c] Copyright 2020, The Authors, published by Wiley-VCH GmbH. II) Microporous hydrogels fabricated by assembling microfiber gels could stimulate the infiltration of host cells and tissue into the hydrogel after subcutaneous implantation. (III,IV) Microporous hydrogels fabricated by assembling microfiber gels could enhance cartilage regeneration and implant integration with host tissue after being injected into articular cartilage defects of rats. II–IV) Reproduced with permission.^[20] Copyright 2022, Wiley-VCH GmbH.

microgels for in vitro cartilage regeneration. Recently, our group developed a microporous hydrogel from SA/MeHA composite microfiber gels produced by wet spinning, which were subsequently crosslinked to form bulk SA/MeHA hydrogels for cartilage regeneration.^[20] As this method facilitates the incorporation of bioactive substances, stem cell-derived exosomes were incorporated into the hydrogel to regulate host inflammation and recruit bone marrow mesenchymal stem cells (BMMSCs). In addition, PLGA microspheres containing kartogenin (KGN) (PLGA_{KGN}) were encapsulated within the hydrogel to induce chondrogenic differentiation of recruited BMMSCs. This design resulted in a bioactive and microporous SA/HA_{exo}-PLGA_{KGN} hydrogel. When tested in vitro, the hydrogel showed sequential release of loaded bioactive substances which collectively induced macrophages to polarize into the anti-inflammatory M2 phenotype, stimulated the migration and infiltration of BMMSCs, and promoted chondrogenic differentiation of the infiltrated BMMSCs toward a chondrocyte phenotype.^[20] In addition, subcutaneous implantation in mice indicated that the micro-

porous structure of the hydrogels facilitated the infiltration of host cells and tissue into the hydrogel structure (Figure 10II). The ability of these hydrogels to induce orthotopic cartilage repair was then tested in vivo by injecting SA/HA_{exo}-PLGA_{KGN} microporous hydrogels in rat articular cartilage defects, compared to other groups of microporous hydrogels that only carried one type of bioactive material (exosomes or KGN) or no bioactive materials. As shown in (Figure 10III), the SA/HA_{exo}-PLGA_{KGN} group showed the best cartilage regeneration at all three-time points. Hematoxylin and eosin (H&E) staining suggested that the SA/HA_{exo}-PLGA_{KGN} microporous hydrogels could enhance integration between the implanted hydrogels and host tissue, as well as increase the number of chondrocytes in the newly formed cartilage tissue, leading to enhanced cartilage regeneration (Figure 10IV). In addition, the SA/HA_{exo}-PLGA_{KGN} hydrogel was found to modulate the in vivo inflammation microenvironment within the cartilage defects and stimulate the deposition of collagen II to assist cartilage formation.

4.2. Application of Microporous Hydrogels Made of Non-spherical Microgels in Smooth Muscle Regeneration

4.2.1. Challenges of Existing Smooth Muscle Repair Techniques

Smooth muscle is found throughout the body, constituting much of the musculature of internal organs and the digestive system.^[49] It is composed of thin, elongated smooth muscle cells that lie parallel to one another in one direction for its contractile function.^[24c] To treat diseases caused by smooth muscle loss, cell-based therapy and tissue engineering have been used to promote smooth muscle regeneration. However, cell-based therapy alone is not able to guide cell alignment and fails to induce the formation of biomimetic-aligned muscle structures, which is critical for the contractile function of smooth muscle. Tissue engineering strategies can use aligned substrates to guide cell alignment, such as electrospun nanofiber membranes with aligned nanofibers which have been commonly applied in smooth muscle regeneration.^[49,50] However, the electrospinning process usually involves solvents and chemicals, thus requiring cells to be post-seeded since cells cannot be encapsulated within the substrate during membrane fabrication. Moreover, electrospun nanofiber membranes usually have limited porosity and small pores, which significantly hinder cell penetration into the membrane and reduce the uniformity of cell distribution. The thickness of electrospun membranes is also limited, making it difficult to regenerate 3D tissues from a sheet-like structure.^[51] Thus, existing strategies for smooth muscle repair face numerous challenges, driving the demand for an ideal scaffold that has the following capabilities: guide cell alignment and stimulate 3D tissue formation, directly encapsulate cells during scaffold fabrication, be easily made on a scale suitable for tissue regeneration (cm scale), have macroporosity to facilitate diffusion of nutrients and metabolic waste, permit infiltration and distribution of cells, and maintain cell viability and proliferation.^[24c,49]

4.2.2. Microporous Hydrogels for Smooth Muscle Regeneration

Hydrogels have favorable characteristics for smooth muscle regeneration, being highly biocompatible and offering the ability to directly encapsulate cells as well as being easily fabricated on the tissue scale. However, they have been seldom considered for this purpose as traditional homogeneous nanoporous hydrogels cannot provide guidance for cell alignment and restrict cell penetration and migration. Recently, the emergence of granular microporous hydrogels, particularly those made of high-aspect-ratio microgels has provided a new option that can satisfy all desirable characteristics of a scaffold for smooth muscle repair, including microporosity and the ability to allow direct cell encapsulation, guidance to cell alignment and tissue formation in 3D, and easy fabrication on the tissue scale.

In the only study so far applying microporous hydrogels made from high-aspect-ratio microgels to smooth muscle regeneration, Lee et al. used gelatin-based microribbon (μ RB) hydrogels with aligned microribbons to culture smooth muscle cells.^[24c] The hydrogel scaffold was found to facilitate cell proliferation, new matrix deposition, and nutrient diffusion. With aligned microribbons within the hydrogel, the hydrogel scaffolds could guide

the alignment of smooth muscle cells and enhance cell adhesion and viability. Moreover, they supported the retention of smooth muscle contractile phenotype after cells were cultured for 7 (Figure 11I-A) and 21 d (Figure 11I-B), as well as accelerated the deposition of smooth muscle ECM proteins collagen I (red, Figure 11I-C) and collagen IV (green Figure 11I-D). The newly deposited collagen was seen to be guided by the aligned microribbons in the hydrogel and presented with the same alignment direction in 3D, mimicking native ECM organization in smooth muscle tissue. In contrast, the newly synthesized collagen within traditional nanoporous hydrogels only deposited around cells without any specific alignment, as cell activity was impeded by homogeneous nanoporosity in the hydrogel structure (Figure 11I-C,D).

4.3. Application of Microporous Hydrogels Made of Non-spherical Microgels in Other Types of Tissue Regeneration

A limited number of studies have applied microporous hydrogels comprising microribbons to bone regeneration. Barati et al. fabricated PLGA into microribbon-shaped building blocks using microcontact printing.^[34] These microribbon building blocks were then coated with fibrinogen to enhance solubility and injectability in aqueous solution. After mixing with thrombin, the fibrinogen-coated PLGA microribbons were inter-crosslinked into 3D hydrogel scaffolds. These hydrogels were used for culturing MSCs and supported homogeneous cell encapsulation, robust cell spreading, and proliferation over 3 d. When the cells were cultured within the hydrogels in an osteogenic medium for 28 d, they showed a significant increase in the levels of early and late markers of bone formation, including alkaline phosphatase expression, collagen deposition, and mineralization (Figure 11II). In addition, the study found that the compressive modulus of MSC-seeded hydrogel scaffolds significantly increased at the same time as bone ECM deposition. The findings indicated that the PLGA μ RB-based hydrogel scaffolds stimulated the differentiation of MSCs toward osteogenesis.

Conrad et al. also fabricated gelatin-based μ RB hydrogel scaffolds with a broad range of stiffness values by varying the degree of hydrogel crosslinking. When MSCs were cultured in these hydrogels, all groups did not affect MSC osteogenesis although they all supported cell spreading, upregulation of osteogenic and mechanosensing markers, and extensive collagen deposition.^[38b] However, the MSC-containing soft μ RB group could not maintain structural integrity and contracted into a small dense cell pellet after 31 d of in vitro culture as they were not able to resist the contractile forces of encapsulated MSCs.

5. Conclusion and Perspectives

Microporous hydrogels have recently attracted increasing research interest due to their improved properties compared to traditional nanoporous hydrogels. The current evidence shows that microporous hydrogels used as cell delivery systems or cell-loaded scaffolds for in vitro tissue engineering can improve the viability and proliferation of encapsulated cells. This is due to their ability to enhance the diffusion of oxygen, nutrients, and

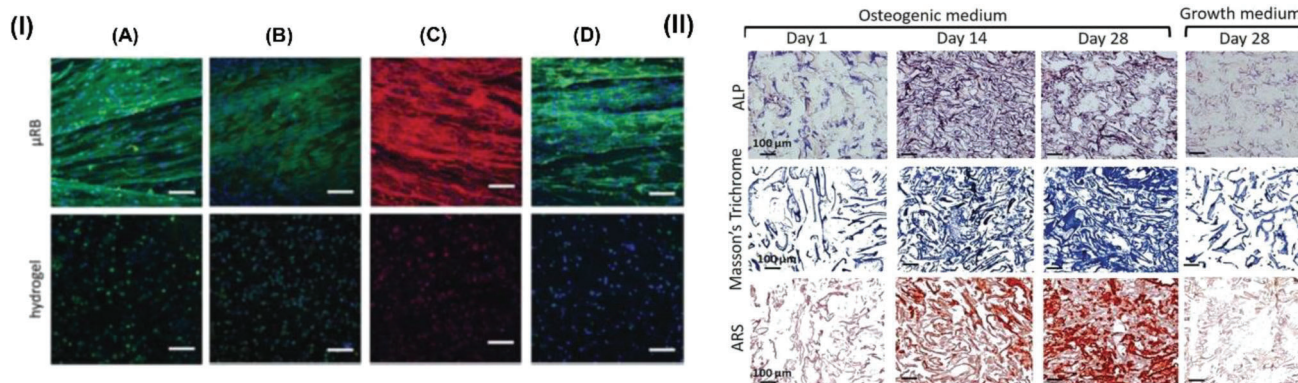


Figure 11. The applications of microporous hydrogels in smooth muscle and bone regeneration. I) Immunostaining of myosin heavy chain (MHC) in both aligned μ RB scaffolds (top row) and traditional hydrogels. Scale bar: 100 μ m. Reproduced with permission.^[24c] Copyright 2016, Wiley-VCH GmbH. II) PLGA μ RB scaffolds support robust bone formation by MSCs in 3D when cultured in osteogenic differentiation medium. Reproduced with permission.^[34] Copyright 2020, Wiley-VCH GmbH.

waste products through their large pore sizes, which also release the encapsulated cells from the restraint of nanopores present in traditional hydrogels. When used as biomaterial scaffolds for *in vivo* tissue engineering, microporous hydrogels can enhance the migration and infiltration of endogenous cells and tissues into the hydrogel structure. In addition to these structural advantages, microporous hydrogels allow easy incorporation of bioactive substances to further accelerate tissue regeneration by providing biological or chemical signals. Among different microgel shapes used to build microporous hydrogels, the non-spherical microgels particularly high-aspect-ratio microgels display distinct advantages over spherical microgels in enhancing mechanical stability and shape fidelity of the resulting bulk hydrogels, improving hydrogel macroporosity, and providing guidance to cell alignment especially for the regeneration of anisotropic tissues.

Diverse techniques are available for producing non-spherical microgels, with microgel assembly being one of the popular methods. The choice of microgel fabrication technique depends on the properties of raw materials, availability of equipment, crosslinking methods, and the scale-up potential of the technique. Among existing techniques, wet spinning demonstrates significant promise due to the ability to control the size of the resulting microfiber or microstrand gels, as well as low requirements for fabrication conditions involving a simple process and low-cost equipment, and high scale-up potential. In addition, fabrication by wet spinning is friendly to the incorporation of bioactive molecules and cells within the hydrogel as it does not involve high voltage, chemicals, oils, or organic solvents. This method can also be used to produce composite microgels or microporous hydrogels with more than one component, demonstrating its application potential in the regeneration of complex or hierarchical tissues. One of the challenges faced by existing microgels fabricated using any method is their limited injectability, since they are either formed under a specific crosslinking environment that does not mimic the wound site or need to be post-treated for further crosslinking. Thus, it is crucial to develop materials and methods for producing microgels that can be further crosslinked in a physiological environment to obtain a reliable method of fabricating injectable microporous hydrogels.

Regarding the physicochemical properties of the microporous hydrogels, current investigations are usually limited to reporting their injectability, porous structure, compression strength, and mechanical stability. To better understand the effects of microgels on the properties of the resulting microporous hydrogels, future studies should characterize the elasticity, resistivity, and relaxation properties of different microgels. Additionally, it would be useful to investigate hydrogel anisotropy in relation to perfusability, flow resistivity, diffusion, and mechanical properties, to better elucidate the mechanisms by which the anisotropic microporous structure of hydrogels affects medium transportation, cell behavior, and cell/tissue infiltration. The effects of porous structure of tissue engineering scaffolds on cell behavior are well established in the literature. However, the specific effects of hydrogel structure in the wet and dry states on cell behavior remain to be systematically clarified. Studies investigating the biological effects of hydrogels routinely freeze dry the hydrogel for performing cell experiments. However, the freeze-drying process changes the pore geometry of hydrogels since nanoscale pores are usually found in as-obtained wet hydrogels while freeze dried hydrogels have microscale pores. Previously, no methods were available to fabricate wet hydrogels with different sizes of microscale pores, making it difficult to understand the effects of the porous structure of wet hydrogels on cell behavior and the mechanisms by which wet hydrogels stimulate tissue regeneration. Through the recent emergence of microporous hydrogel fabrication methods, particularly incorporating different shapes of microgels and pore structure, new options are now available to study the effects of microscale hydrogel pores on cell behavior and to guide rational hydrogel design. However, limited studies are available on this topic and more in-depth investigations are warranted. Moreover, within hydrogels comprising high-aspect-ratio microgels such as microribbons and microfibers, the gaps between microgels are usually tortuous in shape. Although these gaps are sufficiently wide to enable the movement of cells, cell migration may nevertheless be affected by the tortuosity of the porous structures. Further investigation of this relationship would lead to better understanding of the mechanisms by which microporous hydrogels stimulate anisotropic tissue regeneration.

The degradation behavior of microporous hydrogels is critical for their applications in tissue regeneration. Microporous hydrogels, especially those made from microgel assembly, are expected to have different degradation behavior compared to nanoporous hydrogels of the same composition since degradation is likely to begin from the disassembly of microgels. However, most of the existing studies on microporous hydrogels have overlooked the evaluation of biodegradation. Another critical problem is that the majority of current microporous hydrogels have relatively simple spatial and temporal structure. However, tissue regeneration processes typically consist of multiple distinct but continuous stages, including hemostasis, inflammation, proliferation, and maturation, which are physiologically coordinated to occur in a spatially and temporally controlled manner to ensure optimal tissue regeneration.^[44] Unfortunately, current microporous hydrogel designs lack sophisticated strategies for progressing through multiple wound-healing stages in a physiologically relevant manner. To closely recapitulate native tissue healing, it is important to endow microporous hydrogels with the capability for sequential delivery of bioactive molecules targeting each wound healing stage, possibly by creating gradient structures after in situ crosslinking of the constituent microgels. For instance, cells and/or growth factors can be localized in different areas of the hydrogel and delivered at certain stages of wound healing to sequentially modulate inflammation, stimulate the proliferation of cells, and adjust tissue remodeling. Assembling microgels incorporating different preproteins or made from different materials can also give rise to gradient microporous hydrogels with advanced properties.

As shown in this review, microporous hydrogels made of nonspherical microgels show significant promise in regenerating anisotropic tissues and have distinct advantages over hydrogels made of spherical microgels or traditional nanoporous hydrogels. However, their usefulness and practicality in physiologically relevant tissue regeneration need to be further verified in animal models. Most current studies reported the fabrication process of hydrogels and demonstrated their in vitro application in regenerating various types of anisotropic tissues. For example, studies on regenerating articular cartilage using microporous hydrogels with high-aspect-ratio microgels mostly only evaluated the ability of hydrogels to induce tissue formation in vitro. However, there are huge differences between the in vitro and in vivo microenvironment, in particular the dynamic forces experienced during in vivo tissue regeneration are not recapitulated by in vitro models, which is especially important considering the types of tissue regeneration that have been currently attempted in this topic area (cartilage, smooth muscle, and bone). To practically evaluate the effectiveness of using microporous hydrogels for tissue regeneration with a view to enabling future clinical translation, it is necessary to use larger and/or more physiologically relevant animal models, and to study long-term healing responses. In addition, although current studies suggest that the microporous hydrogels can absorb shock during compression testing, most of the hydrogels can only just meet the mechanical requirements for regenerating soft tissue, such as skin and cartilage. New strategies need to be developed for fabricating microporous hydrogels with suitable mechanical properties for supporting other types of tissue regeneration, especially hard tissues, possibly partly through the discovery of new biomaterials instead of the popularly cho-

sen naturally derived materials in current studies such as HA, SA, and gelatin.

Among the limited number of studies that performed testing in small animals to show the advantages of microporous hydrogels, the majority only assessed the structural and biochemical characteristics of the tissue rather than their functional properties. For instance, studies evaluating articular cartilage regeneration using microporous hydrogels usually only assess the histological structure and biochemical markers of the newly formed tissue rather than comparing its mechanical and wear properties with native cartilage. In addition, in vivo studies in large animals are mostly missing, which is a critical step to enable the translation of the hydrogels into clinical applications. For microporous hydrogels comprising non-spherical microgels, all of their current applications have been in the regeneration of musculoskeletal tissues, which have demonstrated advantages in directing cell alignment and differentiation, and in having stable mechanical properties. However, their potential application in the regeneration of other types of anisotropic tissues, particularly soft tissues such as neural tissue, skin, and most internal organs remains to be explored.

This paper has focused on the fabrication and tissue regeneration applications of microporous hydrogels, particularly those composed of nonspherical high-aspect-ratio microgels. However, these microporous hydrogels also have great potential in drug delivery, possibly offering the capability of adjusting drug release behavior with their tunable structure and degradation behavior. In addition, the development and applications of high-aspect-ratio microgels as bioinks for 3D bioprinting to create advanced in vitro cell culture platforms, organ-on-a-chip systems, or hierarchical bioprinted tissue organoids pose exciting areas of future development.

Acknowledgements

This work was supported by the RMIT Vice-Chancellor's Senior Research Fellowship 2020. K.S.L. acknowledges RMIT HDR Scholarship and L.B. acknowledges Australian Research Council Discovery Early Career Researcher Fellowship (DE190101514).

Open access publishing facilitated by RMIT University, as part of the Wiley - RMIT University agreement via the Council of Australian University Librarians.

Conflict of Interest

The authors declare no conflict of interest.

Keywords

granular hydrogels, microgels, microporous hydrogels, tissue regeneration

Received: May 18, 2023

Revised: July 3, 2023

Published online:

[1] a) E. M. Ahmed, *J. Adv. Res.* **2015**, *6*, 105; b) Q. Chai, Y. Jiao, X. Yu, *Gels* **2017**, *3*, 6.

- [2] T. H. Qazi, D. J. Mooney, G. N. Duda, S. Geissler, *Biomaterials* **2017**, *140*, 103.
- [3] X. Sun, S. Agate, K. S. Salem, L. Lucia, L. Pal, *ACS Appl. Bio Mater.* **2021**, *4*, 140.
- [4] a) J. Li, D. J. Mooney, *Nat. Rev. Mater.* **2016**, *1*, 16071; b) M. Vigata, C. Meinert, D. W. Hutmacher, N. Bock, *Pharmaceutics* **2020**, *12*, 1188.
- [5] a) Y. Chao, Q. Chen, Z. Liu, *Adv. Funct. Mater.* **2020**, *30*, 1902785; b) X. Xue, Y. Hu, Y. Deng, J. Su, *Adv. Funct. Mater.* **2021**, *31*, 2009432.
- [6] a) P. Zarrintaj, M. Khodadadi Yazdi, M. Youssefi Azarfam, M. Zare, J. D. Ramsey, F. Seidi, M. Reza Saeb, S. Ramakrishna, M. Mozafari, *Tissue Eng., Part A* **2021**, *27*, 821; b) M. Liu, X. Zeng, C. Ma, H. Yi, Z. Ali, X. Mou, S. Li, Y. Deng, N. He, *Bone Res.* **2017**, *5*, 17014; c) J. H. Lee, *Biomater. Res.* **2018**, *22*, 27; d) B. Peña, M. Laughter, S. Jett, T. J. Rowland, M. R. G. Taylor, L. Mestroni, D. Park, *Macromol. Biosci.* **2018**, *18*, 1800079; e) K. Nagahama, T. Ouchi, Y. Ohya, *Adv. Funct. Mater.* **2008**, *18*, 1220; f) T. Birman, D. Seliktar, *Adv. Funct. Mater.* **2021**, *31*, 2100628; g) Y. Dong, A. Sigen, M. Rodrigues, X. Li, S. H. Kwon, N. Kosaric, S. Khong, Y. Gao, W. Wang, G. C. Gurtner, *Adv. Funct. Mater.* **2017**, *27*, 1606619.
- [7] a) S. J. Hollister, *Nat. Mater.* **2005**, *4*, 518; b) A. C. Sutarin, A. J. D. Krüger, K. Neidig, N. Klos, N. Dolfen, M. Bund, T. Gronemann, R. Sebers, A. Manukanc, G. Yazdani, Y. Kittel, D. Rommel, T. Haraszti, J. Köhler, L. De Laporte, *Adv. Healthcare Mater.* **2022**, *11*, 2200989; c) P. Wang, X. Meng, R. Wang, W. Yang, L. Yang, J. Wang, D.-A. Wang, C. Fan, *Adv. Healthcare Mater.* **2022**, *11*, 2102818.
- [8] a) F. B. Coulter, R. E. Levey, S. T. Robinson, E. B. Dolan, S. Deotti, M. Monaghan, P. Dockery, B. S. Coulter, L. P. Burke, A. J. Lowery, R. Beatty, R. Paetzold, J. J. Prendergast, G. Bellavia, S. Straino, F. Cianfarani, M. Salamone, C. M. Bruno, K. M. Moerman, G. Gherzi, G. P. Duffy, E. D. O’Cearbhaill, *Adv. Healthcare Mater.* **2021**, *10*, 2100229; b) N. J. Darling, W. Xi, E. Sideris, A. R. Anderson, C. Pong, S. T. Carmichael, T. Segura, *Adv. Healthcare Mater.* **2020**, *9*, 1901391; c) N. Annabi, J. W. Nichol, X. Zhong, C. Ji, S. Koshy, A. Khademhosseini, F. Dehghani, *Tissue Eng., Part B* **2010**, *16*, 371; d) C. Ji, A. Khademhosseini, F. Dehghani, *Biomaterials* **2011**, *32*, 9719.
- [9] a) H. Cao, L. Duan, Y. Zhang, J. Cao, K. Zhang, *Signal Transduction Targeted Ther.* **2021**, *6*, 426; b) A. Leal-Egaña, U.-D. Braumann, A. Díaz-Cuencua, M. Nowicki, A. Bader, *J. Nanobiotechnol.* **2011**, *9*, 24.
- [10] D. Sengupta, S. D. Waldman, S. Li, *Ann. Biomed. Eng.* **2014**, *42*, 1537.
- [11] a) N. T. Saidu, A. Fernández-Colino, B. S. Heidari, R. Kent, M. Vernon, O. Bas, S. Mulderrig, A. Lubig, J. C. Rodríguez-Cabello, B. Doyle, D. W. Hutmacher, E. M. De-Juan-Pardo, P. Mela, *Adv. Funct. Mater.* **2022**, *32*, 2110716; b) A. N. Steele, L. M. Stapleton, J. M. Farry, H. J. Lucian, M. J. Paulsen, A. Eskandari, C. E. Hironaka, A. D. Thakore, H. Wang, A. C. Yu, D. Chan, E. A. Appel, Y. J. Woo, *Adv. Healthcare Mater.* **2019**, *8*, 1801147.
- [12] a) F. X. Zhang, P. Liu, W. Ding, Q. B. Meng, D. H. Su, Q. C. Zhang, R. X. Lian, B. Q. Yu, M. D. Zhao, J. Dong, Y. L. Li, L. B. Jjiang, *Biomaterials* **2021**, *278*, 121169; b) R. Dimatteo, N. J. Darling, T. Segura, *Adv. Drug Delivery Rev.* **2018**, *127*, 167.
- [13] G. Ying, N. Jjiang, C. Parra-Cantu, G. Tang, J. Zhang, H. Wang, S. Chen, N. P. Huang, J. Xie, Y. Zhang, *Adv. Funct. Mater.* **2020**, *30*, 2003740.
- [14] a) R.-S. Hsu, P.-Y. Chen, J.-H. Fang, Y.-Y. Chen, C.-W. Chang, Y.-J. Lu, S.-H. Hu, *Adv. Sci.* **2019**, *6*, 1900520; b) Q. Feng, D. Li, Q. Li, X. Cao, H. Dong, *Bioact. Mater.* **2022**, *9*, 105; c) T. H. Qazi, J. A. Burdick, *Biomater. Biosyst.* **2021**, *1*, 100008.
- [15] a) B. Conrad, L. H. Han, F. Yang, *Tissue Eng., Part A* **2018**, *24*, 1631; b) L. Riley, L. Schirmer, T. Segura, *Curr. Opin. Biotechnol.* **2019**, *60*, 1.
- [16] a) C. Gegg, F. Yang, *Acta Biomater.* **2020**, *101*, 196; b) D. M. Headen, J. R. García, A. J. García, *Microsyst. Nanoeng.* **2018**, *4*, 17076; c) H. Rogan, F. Ilagan, X. Tong, C. R. Chu, F. Yang, *Biomaterials* **2020**, *228*, 119579.
- [17] T. H. Qazi, J. Wu, V. G. Muir, S. Weintraub, S. E. Gullbrand, D. Lee, D. Issadore, J. A. Burdick, *Adv. Mater.* **2022**, *34*, 2109194.
- [18] X. Zhang, Y. Li, D. He, Z. Ma, K. Liu, K. Xue, H. Li, *Chem. Eng. J.* **2021**, *425*, 130677.
- [19] a) T. H. Qazi, V. G. Muir, J. A. Burdick, *ACS Biomater. Sci. Eng.* **2022**, *8*, 1427; b) L. R. Nih, E. Sideris, S. T. Carmichael, T. Segura, *Adv. Mater.* **2017**, *29*, 1606471.
- [20] Z. Ma, W. Song, D. He, X. Zhang, Y. He, H. Li, *Adv. Funct. Mater.* **2022**, *32*, 2113380.
- [21] a) X. Zhang, Y. Li, Z. Ma, D. He, H. Li, *Bioact. Mater.* **2021**, *6*, 3692; b) A. Lueckgen, D. S. Garske, A. Ellinghaus, D. J. Mooney, G. N. Duda, A. Cipitria, *Biomaterials* **2019**, *217*, 119294; c) S. Hou, R. Lake, S. Park, S. Edwards, C. Jones, K. J. Jeong, *ACS Appl. Bio Mater.* **2018**, *1*, 1430; d) K. T. Campbell, R. S. Stilhano, E. A. Silva, *Biomaterials* **2018**, *179*, 109; e) K. M. Galler, L. Aulisa, K. R. Regan, R. N. D’Souza, J. D. Hartgerink, *J. Am. Chem. Soc.* **2010**, *132*, 3217; f) X. Kong, L. Chen, B. Li, C. Quan, J. Wu, *J. Mater. Chem. B* **2021**, *9*, 2785; g) S. Reakasame, A. R. Boccaccini, *Biomacromolecules* **2018**, *19*, 3; h) A. Lueckgen, D. S. Garske, A. Ellinghaus, R. M. Desai, A. G. Stafford, D. J. Mooney, G. N. Duda, A. Cipitria, *Biomaterials* **2018**, *181*, 189; i) M. P. Lutolf, J. L. Lauer-Fields, H. G. Schmoekel, A. T. Metters, F. E. Weber, G. B. Fields, J. A. Hubbell, *Proc. Natl. Acad. Sci. USA* **2003**, *100*, 5413.
- [22] a) Z. Jiang, F. Y. Lin, K. Jiang, H. Nguyen, C. Y. Chang, C. C. Lin, *Biomater. Adv.* **2022**, *134*, 112712; b) H. Aksel, D. Sarkar, M. H. Lin, A. Buck, G. T. Huang, *J. Endod.* **2022**, *48*, 527; c) D. Suzuki, C. Kobayashi, *Langmuir* **2014**, *30*, 7085; d) D. Rommel, M. Mork, S. Vedaraman, C. Bastard, L. P. B. Guerzoni, Y. Kittel, R. Vinokur, N. Born, T. Haraszti, L. De Laporte, *Adv. Sci.* **2022**, *9*, 2103554.
- [23] a) G. Bao, T. Jiang, H. Ravanbakhsh, A. Reyes, Z. Ma, M. Strong, H. Wang, J. M. Kinsella, J. Li, L. Mongeau, *Mater. Horiz.* **2020**, *7*, 2336; b) S. Taheri, G. Bao, Z. He, S. Mohammadi, H. Ravanbakhsh, L. Lessard, J. Li, L. Mongeau, *Adv. Sci.* **2022**, *9*, 2102627.
- [24] a) L.-H. Han, S. Yu, T. Wang, A. W. Behn, F. Yang, *Adv. Funct. Mater.* **2013**, *23*, 346; b) Z. Jiang, B. Xia, R. McBride, J. Oakey, *J. Mater. Chem. B* **2017**, *5*, 173; c) S. Lee, X. Tong, L. H. Han, A. Behn, F. Yang, *J. Biomed. Mater. Res. A* **2016**, *104*, 1064.
- [25] a) A. Leferink, D. Schipper, E. Arts, E. Vrij, N. Rivron, M. Karperien, K. Mittmann, C. van Blitterswijk, L. Moroni, R. Truckenmüller, *Adv. Mater.* **2014**, *26*, 2592; b) A. C. Daly, L. Riley, T. Segura, J. A. Burdick, *Nat. Rev. Mater.* **2020**, *5*, 20; c) B. Kessel, M. Lee, A. Bonato, Y. Tinguely, E. Tosoratti, M. Zenobi-Wong, *Adv. Sci.* **2020**, *7*, 2001419.
- [26] a) D. R. Griffin, W. M. Weaver, P. O. Scumpia, D. Di Carlo, T. Segura, *Nat. Mater.* **2015**, *14*, 737; b) J. E. Mealy, J. J. Chung, H. H. Jeong, D. Issadore, D. Lee, P. Atluri, J. A. Burdick, *Adv. Mater.* **2018**, *30*, 1705912; c) Z.-K. Cui, S. Kim, J. J. Baljon, B. M. Wu, T. Aghaloo, M. Lee, *Nat. Commun.* **2019**, *10*, 3523.
- [27] M. Kessler, Q. Nassisi, E. Amstad, *Macromol. Rapid Commun.* **2022**, *43*, 2200196.
- [28] a) J. P. Newsom, K. A. Payne, M. D. Krebs, *Acta Biomater.* **2019**, *88*, 32; b) N. F. Truong, E. Kurt, N. Tahmizyan, S. C. Lesher-Pérez, M. Chen, N. J. Darling, W. Xi, T. Segura, *Acta Biomater.* **2019**, *94*, 160.
- [29] a) S. Salehi, S. Ostrovidov, M. Ebrahimi, R. B. Sadeghian, X. Liang, K. Nakajima, H. Bae, T. Fujie, A. Khademhosseini, *ACS Biomater. Sci. Eng.* **2017**, *3*, 579; b) C. T. Thorpe, H. R. Screen, *Adv. Exp. Med. Biol.* **2016**, *920*, 3.
- [30] a) H. Alzanbaki, M. Moretti, C. A. E. Hauser, *Micromachines* **2021**, *12*, 45; b) M. Karg, A. Pich, T. Hellweg, T. Hoare, L. A. Lyon, J. J. Crassous, D. Suzuki, R. A. Gumerov, S. Schneider, I. I. Potemkin, W. Richtering, *Langmuir* **2019**, *35*, 6231; c) C. S. O’Byrne, T. Bhattacharjee, S. L. Marshall, W. Gregory Sawyer, T. E. Angelini, *Int. J. Bioprint.* **2018**, *11*, e00037.
- [31] a) A. L. Liu, A. J. García, *Ann. Biomed. Eng.* **2016**, *44*, 1946; b) A. Sinclair, M. B. O’Kelly, T. Bai, H. C. Hung, P. Jain, S. Jiang, *Adv. Mater.* **2018**, *30*, 1803087; c) T. Kamperman, M. Karperien, S. Le Gac, J. Leijten, *Trends Biotechnol.* **2018**, *36*, 850; d) C. J. Young, L. A. Poole-Warren, P. J. Martens, *Biotechnol. Bioeng.* **2012**, *109*, 1561; e) D. M.

- Headen, G. Aubry, H. Lu, A. J. García, *Adv. Mater.* **2014**, *26*, 3003; f) J. M. de Rutte, J. Koh, D. Di Carlo, *Adv. Funct. Mater.* **2019**, *29*, 1900071.
- [32] a) W. Jiang, M. Li, Z. Chen, K. W. Leong, *Lab Chip* **2016**, *16*, 4482; b) A. S. Caldwell, G. T. Campbell, K. M. T. Shekro, K. S. Anseth, *Adv. Healthcare Mater.* **2017**, *6*, 1700254; c) A. S. Qayyum, E. Jain, G. Kolar, Y. Kim, S. A. Sell, S. P. Zustiak, *Biofabrication* **2017**, *9*, 025019; d) L. Zhang, K. Chen, H. Zhang, B. Pang, C. H. Choi, A. S. Mao, H. Liao, S. Utech, D. J. Mooney, H. Wang, D. A. Weitz, *Small* **2018**, *17*, 1702955.
- [33] a) S. Xu, Z. Nie, M. Seo, P. Lewis, E. Kumacheva, H. A. Stone, P. Garstecki, D. B. Weibel, I. Gitlin, G. M. Whitesides, *Angew. Chem., Int. Ed. Engl.* **2005**, *44*, 724; b) M. E. Helgeson, S. C. Chapin, P. S. Doyle, *Curr. Opin. Colloid Interface Sci.* **2011**, *16*, 106.
- [34] D. Barati, K. Watkins, Z. Wang, F. Yang, *Small* **2020**, *16*, 1905820.
- [35] H.-H. Jeong, V. R. Yelleswarapu, S. Yadavali, D. Issadore, D. Lee, *Lab Chip* **2015**, *15*, 4387.
- [36] Y. Cheng, Y. Yu, F. Fu, J. Wang, L. Shang, Z. Gu, Y. Zhao, *ACS Appl. Mater. Interfaces* **2016**, *8*, 1080.
- [37] a) M. A. Al Faruque, R. Remadevi, J. M. Razal, M. Naebe, *J. Appl. Polym. Sci.* **2020**, *137*, 49264; b) J. Araki, M. Miyayama, *Polymer* **2020**, *188*, 122116.
- [38] a) C. Gegg, X. Tong, F. Yang, *ACS Biomater. Sci. Eng.* **2020**, *6*, 4166; b) B. Conrad, C. Hayashi, F. Yang, *ACS Biomater. Sci. Eng.* **2020**, *6*, 3454.
- [39] H. Shieh, M. Saadatmand, M. Eskandari, D. Bastani, *Sci. Rep.* **2021**, *11*, 1565.
- [40] O. Bonhomme, J. Leng, A. Colin, *Soft Matter* **2012**, *8*, 10641.
- [41] L. P. B. Guerzoni, J. C. Rose, D. B. Gehlen, A. Jans, T. Haraszti, M. Wessling, A. J. C. Kuehne, L. De Laporte, *Small* **2019**, *15*, 1900692.
- [42] G. C. Le Goff, J. Lee, A. Gupta, W. A. Hill, P. S. Doyle, *Adv. Sci.* **2015**, *2*, 1500149.
- [43] H. Onoe, T. Okitsu, A. Itou, M. Kato-Negishi, R. Gojo, D. Kiriya, K. Sato, S. Miura, S. Iwanaga, K. Kuribayashi-Shigetomi, Y. T. Matsunaga, Y. Shimoyama, S. Takeuchi, *Nat. Mater.* **2013**, *12*, 584.
- [44] Z. Ma, W. Song, Y. He, H. Li, *ACS Appl. Mater. Interfaces* **2020**, *12*, 29787.
- [45] A. J. Sophia Fox, A. Bedi, S. A. Rodeo, *Sports Health* **2009**, *1*, 461.
- [46] R. Chen, J. S. Pye, J. Li, C. B. Little, J. J. Li, *Bioact. Mater.* **2023**, *27*, 505.
- [47] A. R. Martin, J. M. Patel, H. M. Zlotnick, J. L. Carey, R. L. Mauck, *npj Regener. Med.* **2019**, *4*, 12.
- [48] L. Roseti, B. Grigolo, *J. Exp. Orthop.* **2022**, *9*, 61.
- [49] C. M. Garrison, A. Singh-Varma, A. K. Pastino, J. A. M. Steele, J. Kohn, N. S. Murthy, J. E. Schwarzbauer, *J. Biomed. Mater. Res., Part A* **2021**, *109*, 733.
- [50] J. A. Reid, A. McDonald, A. Callanan, *J. Mater. Sci.: Mater. Med.* **2021**, *32*, 131.
- [51] a) B. Yan, Y. Zhang, Z. Li, P. Zhou, Y. Mao, *SN Appl. Sci.* **2022**, *4*, 172; b) L. Muthukrishnan, *Colloid Polym. Sci.* **2022**, *300*, 875.



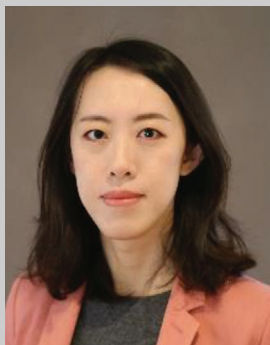
Haiyan Li is currently a vice chancellor's senior research fellow at the Royal Melbourne Institute of Technology (RMIT), Australia. Her career began when she received a Ph.D. degree in materials engineering from Shanghai Institute of Ceramics, Chinese Academy of Sciences in 2005. She has had a varied research career working in both industry (Unilever Investment Co. Ltd) and academia (Monash University, INSERM of France, and Shanghai Jiao Tong University) over the past 18 years. Her research in tissue engineering focuses on developing bioactive materials for in situ regenerating of chronic wound healing, osteochondral, cartilage, and tendon-to-bone healing.



Keerthi Subramanian Iyer is a Ph.D. candidate at RMIT University under the supervision of Dr. Haiyan Li, Dr. Lei Bao, Dr. Jiali Zhai and Dr. Jiao Jiao Li. Her doctoral work focuses on the development of advanced injectable microporous hydrogels for improving tissue regeneration. She holds a Master's degree in nanotechnology engineering from Bharati Vidyapeeth Deemed University, India, and has more than two years of experience in biomaterial synthesis and its application in bioengineering.



Lei Bao currently is a senior lecturer at RMIT University, Australia. She joined RMIT in late 2014 after she completed the endeavour fellowship at the University of Melbourne. She held RMIT vice-chancellor fellowship from 2015 to 2018 and is a recipient of the Australian Research Council Discovery Early Career Researcher Award. Her multidisciplinary work is centered on solving energy, environment, and health-related challenges through controllable design and engineering of nanomaterials. The research team she leads focuses on confined synthesis and assembly of nanomaterials for energy conversions as well as in the development of biocompatible multifunctional nanocomposites for biomedical applications.



Jiali Zhai is a senior research fellow at RMIT University with research interests in developing nanoparticle and hydrogel systems for drug delivery and biomedical applications as well as understanding amphiphile self-assembly at interfaces. Her research also involves employing synchrotron X-ray scattering techniques to understand the kinetics and formation of self-assembled systems in complex environments. She was awarded a Ph.D. in biochemistry by Monash University. She has received several awards including a Victoria Fellowship, an Australasian Colloids and Interface Society Lectureship, and a CSIRO OCE Postdoctoral Fellowship.



Jiao Jiao Li is a senior lecturer in biomedical engineering at University of Technology Sydney (UTS). Her research in regenerative medicine focuses on developing combinatorial approaches including stem cells and biomaterials to treat chronic diseases, particularly bone and joint disorders. She was a National Health and Medical Research Council (NHMRC) Early Career Fellow, co-deputy director on the Australian Research Council Training Centre for Innovative BioEngineering, and a Science & Technology Australia 2021-22 Superstar of STEM.